2011-07-07

Mechanical Characterization of the Interspinous Ligament using Anisotropic Small Punch Testing

Rachel Jane Bradshaw
Brigham Young University - Provo

Mechanical Characterization of the Human Interspinous Ligament using Anisotropic Small Punch Testing

Rachel Jane Bradshaw

A thesis submitted to the faculty of
Brigham Young University
in partial fulfillment of the requirements for the degree of

Master of Science

Anton E. Bowden, Chair
Larry L. Howell
Brent L. Adams

Department of Mechanical Engineering

Brigham Young University

August 2011

ABSTRACT

Mechanical Characterization of the Human Interspinous Ligament using Anisotropic Small Punch Testing

Rachel Jane Bradshaw
Department of Mechanical Engineering
Master of Science

Objective: The objective of this work was to characterize the nonlinear anisotropic material constitutive response of the interspinous ligament (ISL).

Methods: Cadaveric test samples of the interspinous ligament were tested using the anisotropic small punch test. The measured force-displacement response served as experimental input into a system identification optimization routine to determine the constitutive material parameters that replicated the measured material response.

Results: The constitutive behavior of the ISL is notably different from that reported for knee, shoulder, and hip ligaments. Specifically, the high collagen fiber content and unique collagen architecture provided a stiffer material response. The results from the present work were compared with available data from the literature for the ISL and were found to be consistent with reported failure stress and strain to failure.

Conclusion: The ISL has unique constitutive properties and architecture that provide mechanical and clinical stability to the lumbar spine during flexion. The characterization data obtained during accomplishment of this thesis provide valuable insights into these roles. The present work provides a first step to fully characterize and understand both physiological and pathological motion of the spine. Further research is necessary to clarify the contributions of spinal ligaments to spine stability and how damage to spinal ligaments may contribute to chronic lower back pain.

Keywords: Rachel Bradshaw, interspinous ligament, anisotropic small punch tester

ACKNOWLEDGMENTS

I would like to acknowledge the support and guidance of my mentors, collaborators, and family. The guidance of Dr. Anton Bowden has been essential to my development as a researcher over these past two years. I consider him a great friend and am extremely grateful for his mentorship and support. The insights and support of Dr. Larry Howell and Dr. Brent Adams have been most helpful in providing a context for the work and are much appreciated. This research was funded by: National Science Foundation (# CMMI-0952758), Fulton College of Engineering and Technology Supplement Research Grant, BYU Mentor Environment Grant, and a BYU Gerontology Research Grant. This research has also been supported by several collaborators (Dan Robertson, Allison Rankin, Aaron Cannon, Ashu Parajuli, and Chris West) who have been invaluable in facilitating this research. I would also like to thank members of BABEL who have always brought a smile to my face. My parents have always encouraged me to reach beyond my expectations and make a difference in the world. My ten siblings have been the best of friends; with a lifetime of laughter. Finally, I would like to thank my fiancé Luke for his thoughtfulness and unconditional support throughout my studies. Without the help and support of any of these, this work would not be accomplished.

TABLE OF CONTENTS

LIST OF TABLES

LIST OF FIGURES

1 INTRODUCTION

1.1 Problem Statement

The unique microstructure of the interspinous ligament (ISL) generates nonlinear, anisotropic, viscoelastic material responses which have yet to be fully characterized. This void is largely attributed to the inability of traditional uniaxial tensile methods to characterize anisotropy and the inability of in situ methods to isolate individual ligament response. Likewise, the biomechanical testing of isolated tissues often presents additional challenges when gripping ligamentous samples; the minute size of the ISL only exacerbates this issue. Consequently, the contribution of the ISL towards spinal stability and segmental motion remains unclear in both pathological and physiological conditions. The present work developed a multiaxial testing device (ASPT—Anisotropic Small Punch Test) and associated material characterization methodology capable of identifying the nonlinear anisotropic properties of the ISL from cadaver specimens in isolation. The conservative nature of the ASPT only requires very small test samples (6 mm diameter), which facilitated the testing and characterization of multiple samples (n = 1-5) per ISL specimen. The material properties reported for the ISL are suitable for implementation into numerical models of the spine.

1.2 Chapter Summary

Chapter two reviews the anatomy, testing, and characterization of the ISL. First, a review of spinal column anatomy and mechanical functions of its constituents is presented. Next, additional insights on the composition, structure, and properties of ligaments are reviewed. Subsequently, current biomechanical testing and material characterization methods for ligamentous tissues are reviewed. Finally, the functional anatomy, associated pathological conditions, mechanical and neurological roles and biomaterial properties of the ISL are presented.

Chapter three consists of a technical publication, currently under review, which presents the material constitutive characterization of the ISL using the developed testing methodology (ASPT). The contributions and justification of the employed techniques are methods that are discussed in detail; to our knowledge these are the first nonlinear anisotropic material properties to be reported for the ISL.

Chapter four provides additional results and insights regarding the pathology of the ISL and comparison of the derived properties to other material parameters for ligaments in the human body.

Chapter five briefly summarizes the primary contributions of this work and outlines directions for future work that would build on the results presented in this thesis.

2 BACKGROUND

2.1 Lower Back Pain

Lower back pain will affects up to 70-85 % of the population of industrial societies at some point in their lifetime [1]. It is the second most common reason for a doctor visits and the third most common for a surgical procedure [2-4]. It overheads nearly a hundred billion dollars per year in the United States [5-6] and it constitutes 86% of the cost of worker compensation claims—although this only represents 10% of the claims [4]. Predominant pathologies, which are associated with the lower back pain, relate to the following anatomical instabilities: disc herniation, degenerative disc disease, degenerative spondylolisthesis, spinal stenosis degeneration or post-operative instability [7]. For chronic lower back pain the most common treatment is a spinal fusion; however, 68% of patients who undergo this surgery are work disabled two years after the surgery [2]. Alterations in spinal load bearing subsequent to spinal fusion often cause adverse effects to the adjacent segments, accelerating adjacent level disc degeneration [8].

The majority of modern clinical treatment for low back pain is currently focused on treating intervertebral disc pathology. However 64% of people with disc abnormalities claim to have no pain [3]. A component generally ignored, in clinical and research biomechanics, is the contribution of spinal ligaments to spinal stability and potential pathologies associated with ligamentous injuries. A growing amount of evidence links the subfailure of spinal ligaments to

chronic low back pain [1, 9-12]. An additional concern, in relation to the stability of the spine, is that current surgical procedures often cut spinal ligaments [13]. The potential correlation between spinal ligament dysfunction and chronic low back pain is a strong motivator for the present work.

2.2 Spinal Column

The spinal column consists of functionally linked joints comprised of levers (vertebra), pivots (intervertebral discs and facets), passive restraints (ligaments) and actively controlled tension elements (muscles) [14]. Together these systems interact to provide vital anatomical and physiological roles: (1) protection of the spinal cord, nerve roots, and internal organs; (2) support of body weight and physiological motion of the head, trunk and pelvis; (3) scaffold support for the attachment of ligamentous and muscular structures; and (4) hematopoietic production and mineral storage [15]. The spine is classified into five functional areas organized by descending height from the skull: the cervical, thoracic, lumbar, and sacral regions. The cervical and lumbar regions are the most mobile—primarily facilitating flexion and extension—and consequently are most often susceptible to injury [15]. The flexion-extension motion of the thoracic region is constrained by attachment to the rib cage, while the sacral region fuses together during late adolescence and early adulthood. Substantial rotation occurs in the cervical and thoracic regions, while lateral bending primarily occurs in the cervical and lumbar regions.

Natural curvature is exhibited in the sagittal plane in the spinal column of adults, helping counterbalance the loads carried by the spine in neutral standing posture. Kyphosis is defined as an anterior concavity to the spinal curvature, while lordosis is posterior concavity to the spinal curvature. The cervical and lumbar regions exhibit lordosis and the thoracic and sacral regions

exhibit kyphosis. To fully understand the mechanics associated with the spinal column it is essential to understand the anatomical and functional characteristics of all constituents associated with the human spine, both their individual and comprehensive interactions. Consequently, a summary of the characteristics and functions of anatomical structures associated with the spine are discussed in the following sections.

2.2.1 Vertebrae

Vertebrae are the bones of the spinal column which consist of three functional areas which correspond to their relative location. The anterior portion is a massive cylindrical column of bone referred to as the vertebral body. This section functions to provide the primary support of the spinal column and serve as an attachment for the intervertebral disc and provide hematopoietic functions [15]. The size of the vertebral body increases as the spinal column descends inferiorly. In the midsection of the vertebra, the junction of the pedicles and lamina forms the vertebral arch, which in turn forms the walls of the vertebral foramen that houses the spinal cord. Lastly, in the posterior section the vertebra provides seven distinct processes. Four articular processes (2 superior, 2 inferior) provide mechanical restraints on excess spinal motion, particularly in extension and axial rotation. A pair of transverse processes extends laterally from the vertebral arch, while the spinous process extends posteriorly from the vertebral arch. All of the processes serve as ligament and/or muscle attachment points.

2.2.2 Intervertebral Disc

The intervertebral disc is an avascular, flexible cartilaginous joint composed of three distinct sections: the annulus fibrosis, the nucleus pulposus, and the end plate. The disc supports spinal function by resisting excess motion and distributing loads throughout the spinal column.

The annulus fibrosis comprises the outer portion of the intervertebral disc and has a roughly radial symmetry. It is formed of concentric lamina (layers) of proteoglycan matrix/collagen fiber composite. Each lamina alternates angle at approximately +/- 30 degrees from the midplane of the disc [14]. At the core of the disc is the nucleus pulposus, an incompressible gelatinous matrix constrained within the walls of the annulus fibrosus. Together, the nucleus pulposus and the annulus fibrosus, act as a pressure vessel, allowing the spine to support large compressive loads (up to several thousand Newtons). The end plate attaches the disc to the adjacent vertebrae while allowing nutrients to diffuse the disc from the vertebral vasculature [7].

2.2.3 Spinal Ligaments

As shown in Figure 2-1, six spinal ligaments are found at each vertebral joint, consisting of the: anterior longitudinal ligament (ALL), posterior longitudinal ligament (PLL), facet joint capsule (FJC), ligamentum flavum (LF), interspinous ligament (ISL) and supraspinous ligament (SSL). The spinal ligaments collectively form a passive restraint complex which functions in many capacities: (1) guiding a range of physiological spinal motions; (2) providing additional stability while minimizing muscle activation; (3) preventing injury of surrounding spinal components by restricting abnormal motion; and (4) protecting the spinal cord from traumatic injuries under extreme loading conditions [14]. Like other ligaments, spinal ligaments connect bone to bone, specifically attaching adjacent spinal segments together at the vertebral bodies (ALL and PLL), spinous processes (ISL and SSL), facet joints (FJC) and vertebral foramen (LF and PLL).

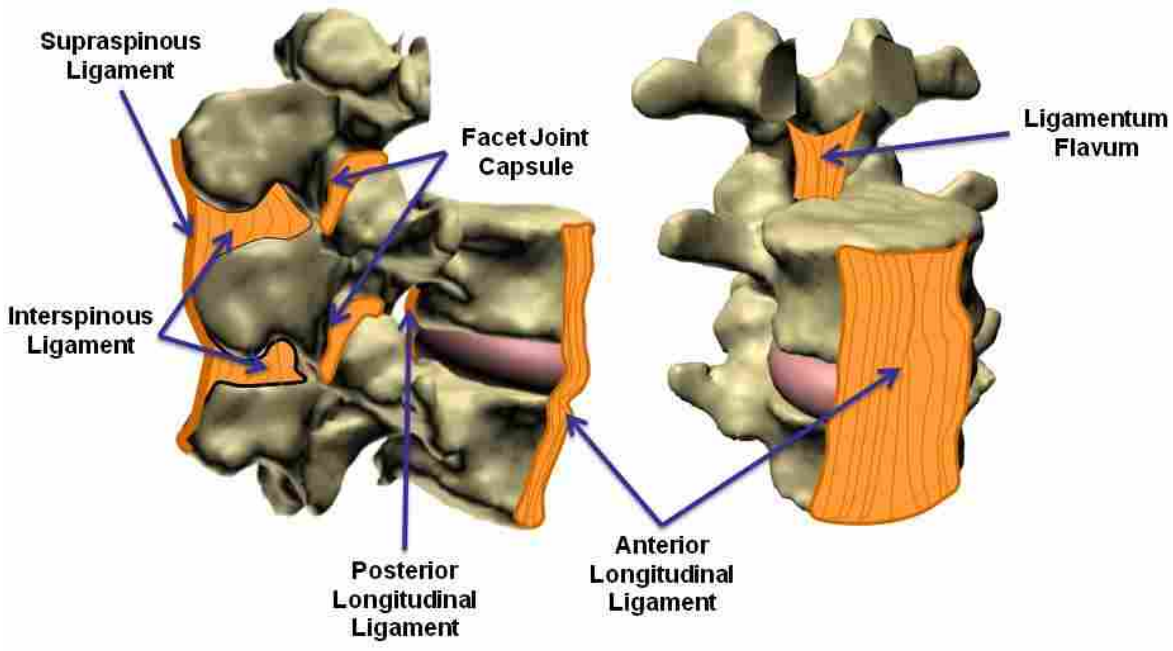

Figure 2-1 Diagram of six spinal ligaments found in the human body

The ALL and PLL extend along the anterior and posterior surfaces (respectively) of the vertebral body along the entire length of the spinal column from the occipital bone to the sacrum. Throughout the length of the spine the ALL attaches narrowly along the vertebral bodies then broadens and inserts into the intervertebral discs [16]. This facilitates the capacity of the spine to resist extension and restricts anterior prolapse of the intervertebral disc. Similarly the PLL resists bending of the spine in flexion, extending along the posterior surface of the vertebral bodies with weaker attachments to the vertebral bodies [17]. Morphological variations in the PLL have been strongly correlated to intervertebral disc herniation [18]. Both the ALL and PLL are reported to have a low elastin content, consisting primarily of several layers of collagen fibrils within a proteoglycan matrix. The high stiffness of these ligaments enables the spinal column to resist sudden loads [19].

In conjunction with the PLL the LF surrounds the vertebral canal. High elastin content in the LF provides significant flexibility, ensuring that the spinal canal does not buckle in flexion or

tear in extension. Although the high elastin content is accompanied by poor directionality of collagen fibers [20] during neutral posture, at higher strains the collagen fibers align and the ligament stiffness increases [19].

Each FJC encapsulates the articular surfaces of the superior and inferior facet joints, forming a synovial joint. The FJC protects the spinal segments from anterior shear, excessive axial rotation and excessive flexion motion. Several injuries are reported with dysfunction of the FJC including: dislocation, inflammation, osteoarthritis, fracture, surgery or other trauma [21].

Both the ISL and SSL insert on to the spinous process, consequently, they are often assumed to be coupled in function and structure are and occasionally studied as an ISL-SSL complex [22-23]. Both become active in the later stages of flexion, resisting hyperflexion and experiencing the highest deformations among all spinal ligaments [24]. The ISL connects the superior and inferior ridges of adjacent spinous processes and inserts into the ventral portion of the LF and dorsally into the SSL. One of the most unique aspects of the ISL is the sigmoidal fiber orientation in the mid-section, which creates a unique loading pathway, which supports 75% of the load in the ISL-SSL complex [25]. The SSL connects to the terminal posterior ends of the spinous process and inserts dorsally into the thorocolumbar fascia. Several controversial reports of the predominance of the SSL report its absence in the lumbar region stating it fuses to the thorocolumbar fascia [16]. However, others distinctly report it to be throughout the entire spinal column [19]. Our observations support the presence of the SSL throughout the lumbar region.

2.2.4 Musculature

Three layers of musculature are defined in the spine: superficial, intermediate and deep. Superficial muscles attach to the trunk and upper limbs to control limb motion. Intermediate

muscles primarily provide proprioceptive functions that assist in providing spinal stability throughout the large range of spinal motion, sensing and reacting to the spatial location of thoracic and lumbar segments [26]. Deep muscles of the back act to control finite motions of the vertebral column and maintain posture [27]. The involvement of abdominal muscles has been reported to be involved in vertebral stability and indirectly produce lumbar flexion [28].

2.2.5 Innervation

The spinal cord descends inferiorly from the base of the brain, providing physical connections of the peripheral nervous systems to the central nervous system. This essential networking path provides communication for virtually all neurological functions which occur in the body. Thirty-one pair of spinal nerve roots exit through the intervertebral foramen of the vertebra comprising the cervical (8), thoracic (12), lumbar (5), sacral (5) and coccygeal (1) nerves. These nerves are networked into highly organized segments known as the brachial plexus and the lumbosacral plexus. Nerves from the brachial plexus branch to innervate the upper extremities, while the lumbosacral plexus innervates the lower abdomen and lower extremities. Additional subdivisions of these branches innervate systems of the body to insure homeostatic conditions are maintained. Of particular interest are the soft tissues associated with the spinal column, specifically intervertebral discs [29-30], spinal ligaments [31-33] and surrounding musculature [34-35], which have each been reported to be involved in proprioceptive functions or motor control for the spine.

2.3 Ligaments

Ligaments are a specialized type of soft connective tissue which connects bone to bone and provides stability and guidance to the kinematic motions of a joint [36]. Ligaments are generally considered to be the primary restrain for most joints, and consequently are frequently damaged in repetitive or sudden motions [37]. Additional evidence suggests that ligaments provide proprioceptive feedback when overstrained or injured. Several human and animal studies have demonstrated that ligament damage not only results in loss of joint stability but is often coupled with chronically increased recruitment of surrounding musculature [38]. When significant injuries occur, damage is often caused to surrounding soft tissues and generally leads to severe pain due to ligomento-muscular instability [39]. Consequently, recent topics in ligament research have included investigation of the mechanisms involved in tissue development [40], histology [41], healing [42], material properties [43], and so forth. Identifying the relationship of structure and function is essential to understanding the fundamental mechanics and ultrastructure of ligaments [44]. Consequently, in the following sections the composition, structure and properties of ligaments are discussed.

2.3.1 Composition

Ligaments are a biological composite material composed of parallel collagen fibers surrounded by an extracellular ground substance matrix. Molecular modeling of collagen fibers has demonstrated the structure's capability to maximize strength while dissipating large amounts of energy [45]. The ground substance matrix includes an array of extracellular constituents which provide sustainable contributions to the collagen scaffold and cellular functionality. However,

close examination of the properties associated with the individual components of ligaments may increase our understanding of their overall biomechanical response.

First, collagen fibers are the most distinctive feature of connective tissue as they are predominately responsible for providing directionality and stability. The superior mechanical properties of collagen have primarily been attributed to the repetitive hierarchal organization of tropocollagen [45]. Tropocollagen, in its most basic unit, consists of three fibrous polypeptides, which self-assemble forming a triple helix structure. Four tropocollagens stagger longitudinally to create a fibril, and numerous fibrils align parallel to one another forming a collagen fiber [46]. Collagen fibers then align along the predominant loading principle axis, allowing tensile loads to transmit across a joint [47].

The ground substance matrix is a gelatinous adhesive responsible for holding collagen fibers in their respective position. It is composed of proteoglycans, water, fibroblasts, and elastin [15]. Proteoglycans sustain physiological conditions by aggregating water molecules within the ligament structure [48]. Two-thirds of the content in ligaments is water and the remaining third is primarily fibrous collagen proteins [35]. Fibroblasts, embedded within the ground substance matrix, function to uphold the collagen scaffold via matrix synthesis [47] Elastin is coiled protein which functions to provide elastic recoil of ligaments, reorganizing the bundle arrangements following ligament deformation [49].

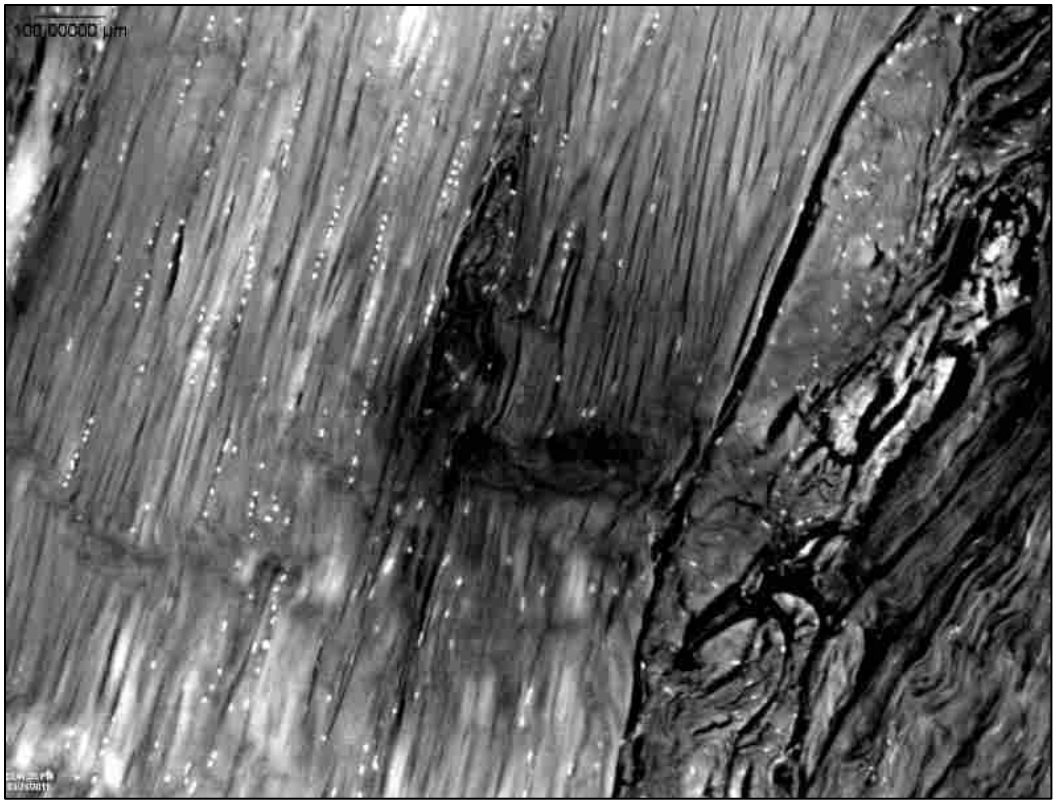

Figure 2-2 A contract microscopic image of the ISL microstructure, showing: the collagen fibers (grey fibers), ground substance matrix (black matrix), and fibroblasts (white dots)

2.3.2 Structure

The structure of ligaments is essential to providing superior strength and resilience to joints throughout the human body. At the microscopic level the structural components of ligaments facilitate complex biomechanical functions, which are adaptable to the mechanical loading environment [44]. Several other aspects such as: geometry, insertion angle, interactions with surrounding tissues, and so forth; also contribute to the nonuniform loading pattern of ligaments [24]. However, three distinctive aspects of ligament structure will be discussed in greater detail: the crimp pattern, insertion sites, and pre-strain.

The crimp pattern is a wave-like configuration which is naturally exhibited in collagen fibers, as shown in Figure 2-3. The origin of this pattern is believed to be related with cross-

linked interactions among the collagen fibers and extracellular matrix [44]. This pattern can be described as a spring in series. When ligaments are subject to tensile forces the crimp pattern allows the ligament to undergo elongation without sustaining permanent damage [36]. Likewise, when subject to higher loads the crimp pattern recruits additional fibers to stiffen the ligament while still guiding the motion of the joint [49]. Consequently, in normal physiological activities, the joint moves easily with no permanent deformation.

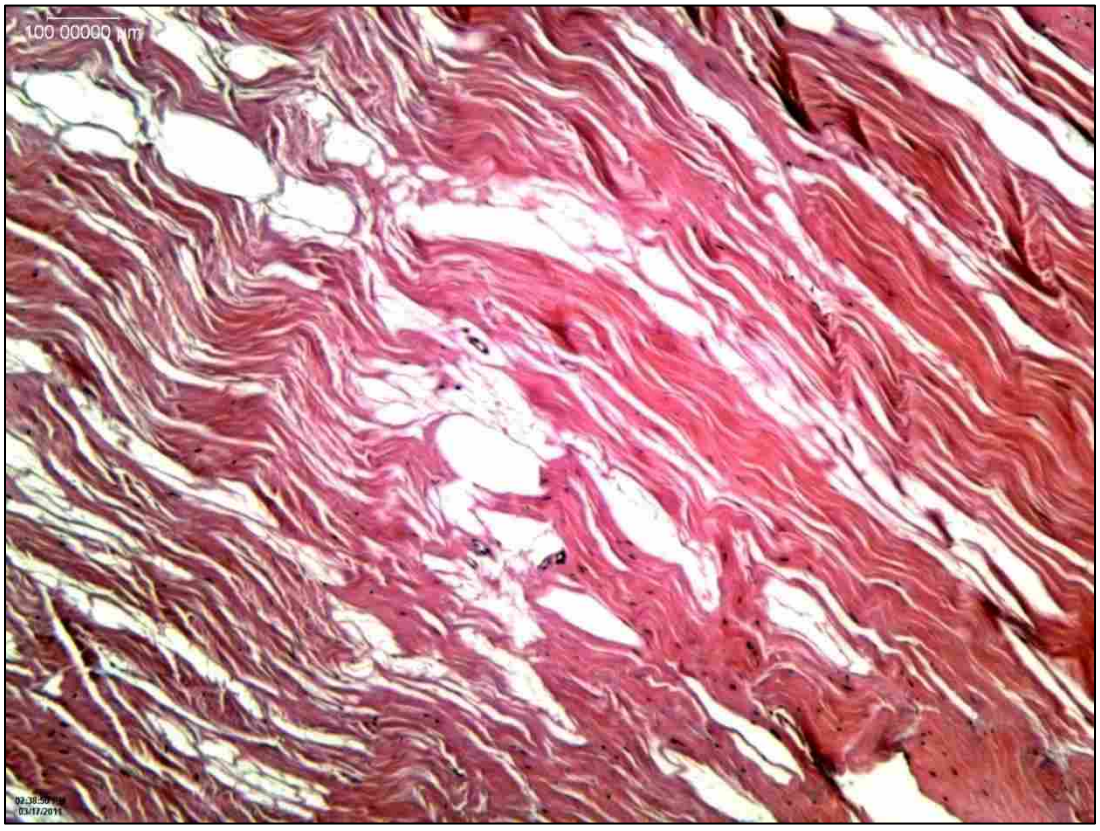

Figure 2-3 A contrast microscopic image of the ISL microstructure showing the crimp pattern

Insertion sites are the attachments which anchor ligaments into bone and transmit stresses experienced by the bone to stresses experienced by the joint [25]. Ligaments insert into bone at unusual shapes on the bones; these geometries are believed to play an important role in how collagen fibers are recruited during joint movement [36]. Two types of insertions exist in the

human body—indirect and direct insertions. Indirect insertions attach ligament to periosteum (a connective tissue membrane that surrounds and attaches to bone) at acute angles, whereas direct insertions gradually transition in composition from ligament to fibrocartilage to mineralize fibrocartilage to bone [50]. The properties of insertion site are not fully understood, but when joints are damaged, insertion site forces have been reported to increase and are associated with joint damage. Failure at the fibrocartilage-bone junction has been reported at the bone suggesting insertion sites may be subject to higher incidences of failure. [51].

In their neutral position, most ligaments still have some tension associated within the joint; this ensures the joint is stable independent of muscle forces [52]. This pre-strain is important to consider when evaluating the biomechanical response of a ligament since it represents pre-existing energy storage that influences stiffness, resilience, and strength. Reports of spinal ligament pre-strain vary widely from 0-19% strain. Computational models that ignore ligament pre-strain can grossly underestimate ligament stress [53].

2.3.3 Biomaterial Properties

As discussed previously, the composition and structure within ligaments are essential to its biomechanical functions. Thus, variations in structure and composition throughout a ligament correspond to material inhomogeneity and associated variations in the material response. This inhomogeneous behavior is challenging to characterize and is exacerbated when comparing the material properties between different ligaments. Additionally, the material response of ligaments is known to be nonlinear, anisotropic, and viscoelastic. [54].

The typical force-deflection curve of ligament tissue has three distinct regions: the toe region (TR), linear region (LR) and ultimate load (UL) [49] (Figure 2-4). The TR is the initial loading of the ligament when the collagen fibers gradually uncrimp. The ligament undergoes

relatively large strains in this region, but does not store very much energy. At the end of the TR, there is a sharp increase in stiffness at the transition point to the LR. This change in stiffness represents the transition from collagen fiber uncrimping to the fully uncrimped tensile stiffness of the fibers. Finally, when a ligament reaches the UL the ligament undergoes permanent deformation and subsequently fails.

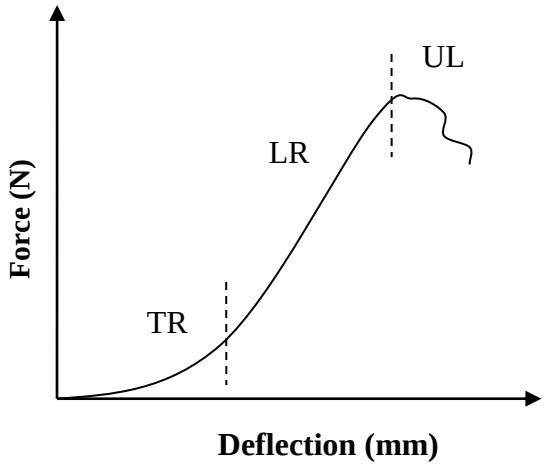

Figure 2-4 Typical force-deflection curve of ligaments showing the toe region (TR), linear region (LR), and ultimate load (UL)

Anisotropy, or directional dependency, is an inherent characteristic of the parallel alignment of the collagen fibers [55]. Many ligaments may be accurately characterized as transversely isotropic [56-58] with a strong response along the direction of the collagen fibers and a weak response perpendicular to the fiber direction. Quapp and Weiss (1998) performed tensile tests on samples from the medial collateral ligament both along and perpendicular to the collagen fibers. These results indicated the tensile strength, ultimate strain, and tangent modulus are significantly higher along the collagen fibers[43]. Several studies have indicated that multiaxial testing data is required in order to fully characterize the anisotropy [49] of ligament material behavior.

Viscoelasticity is the time- and history- dependent response of materials, observed in three forms: stress relaxation, creep, and hysteresis [59] in the stress-strain (or load-deflection) response (Figure 2-6). These properties are observed in ligaments and believed to arise from the interaction of water with constituents in the ground substance matrix [51-52]. Biomechanically, viscoelasticity provides 'load relaxation' in the ligaments that allows the loads to decrease in a ligament when under repetitive cyclic loads, preventing injury [36]. Practically, biomechanical testing of ligaments has revealed that within a few cycles of repetitive testing (termed "preconditioning"), much of the viscoelastic effect has been exhausted, which yields a highly repeatable stress-strain response that follows a consistent hysteresis path. However, after a relatively short (several minutes) rest period, the full viscoelastic effect is restored.

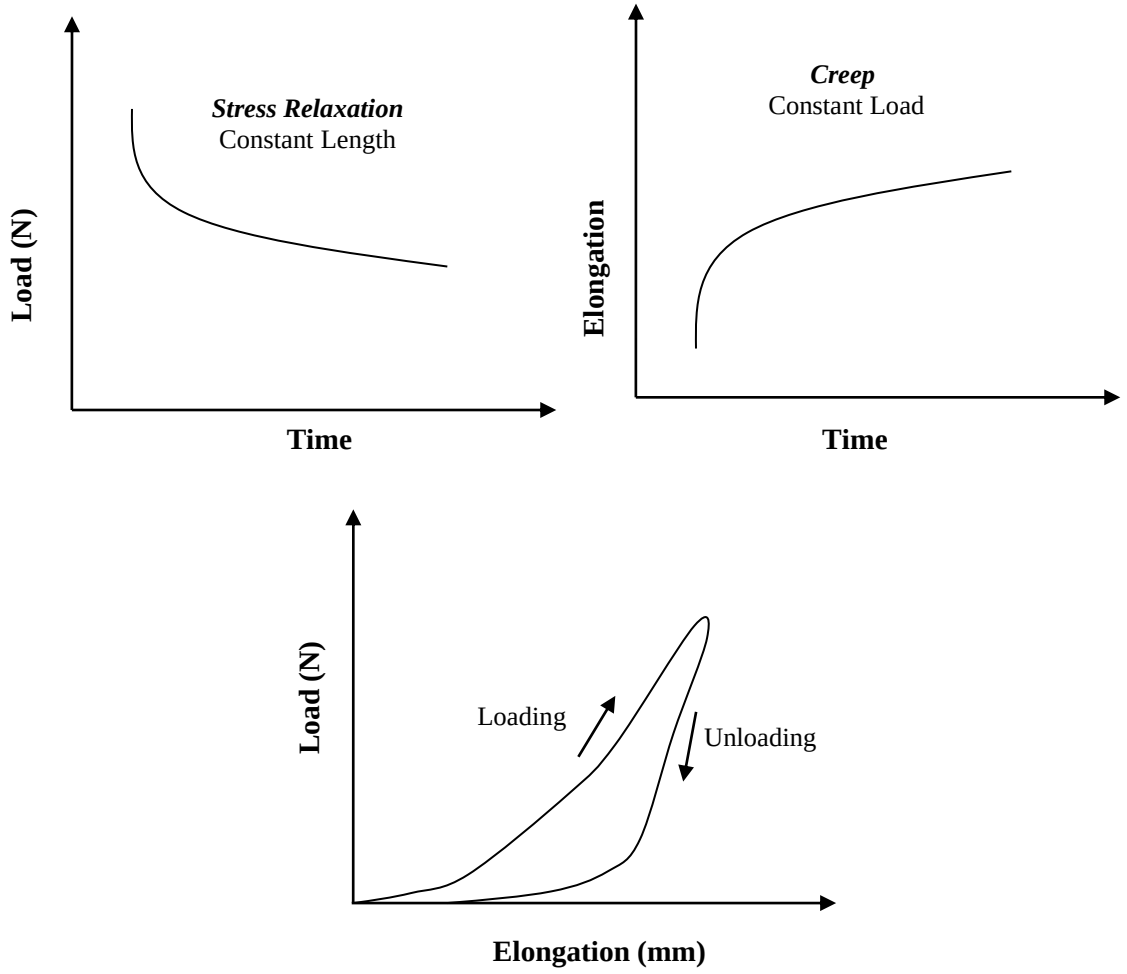

Figure 2-5 Typical viscoelastic behaviors of ligaments: (top left) stress relaxation, (top right) creep, and (bottom) hysteresis

2.4 Biomechanical Testing of Ligaments

Numerous difficulties are associated with the mechanical testing of connective tissues. However, several studies report suggested techniques and solutions which may be implemented to overcome common limitations. The following sections will discuss in greater detail how researchers have resolved these issues in the past.

2.4.1 Tissue Samples

The condition, storage, and handling of a test specimen are essential to ensure that the sample is not damaged. When in the body, ligaments are subject to environmental factors such as remodeling, degeneration or damage; which alter the microstructure [37]. It is important to be aware of any pre-existing conditions that could have damaged the specimen. Likewise, the comparison of properties among different ligament samples will likely have large variety. If a sample is not frozen properly ice crystals will form within the ligament damaging the structure and altering the mechanical response. The number of freeze thaw cycles a sample undergoes should be limited and properly recorded [60]. Some studies resolve these issues by obtaining fresh tissue samples, flash freezing the sample and storing it in a vacuum sealed container [61-62]. It is also vital to keep ligaments hydrated with physiologically buffered saline solution, in regular intervals [63]. Otherwise the sample will dry out and the mechanical properties will drastically alter. Finally, the applied experimental methods such as: preconditioning, loading orientation, testing rate, and testing environment will also play important factors in determining the measured material response.

2.4.2 Measurement Techniques

Accurate geometrical measurements of a sample's cross-sectional area and original length are necessary to calculate the material properties of a ligament [52]. Cross sectional area generally varies considerably along the length of a ligament. Contact methods for measuring ligament geometry include: molding techniques, digital vernier calipers, and area micrometers; but they have gradually been discontinued since they are reported to deform the area of the tissue being measured and give inaccurate measurements [59, 64]. More recently, noncontact methods

have been utilized, including various optical system measurements which do not deform the sample [65-66].

Techniques for tracking ligament strain have also developed over the years. Originally, researchers would use the crosshead displacement of the testing apparatus to determine strain. However, large errors are introduced in this system from an inhomogeneous material response in the ligament, slipping in the clamps, or slack in the testing equipment. Thereafter several researcher fastened pins, strain gauges, beads, or sutures onto the surface of ligaments. Some of these methods are more aggressive and may restrict or alter the strain measured. A calibrated video system with two cameras measure the three-dimensional strain field between each marker pair on the ligament [52]. Likewise noninvasive *in vivo* measurements of soft tissue strain have been reported using tagged magnetic resonance imaging techniques [67].

2.4.3 Testing Methods

Common biomechanical testing methods used to evaluate ligaments include uniaxial and multiaxial tensile testing methods. A common challenge among these methods is establishing a uniform loading condition. The structural properties of ligaments are obtained from load-displacement data and represented by parameters such as: stiffness, ultimate load, and energy absorbed at failure [49]. Material properties of ligaments take geometric measurements (cross sectional area and gauge length) into account which transform load-displacement curves into stress-strain curves; reporting the tangent modulus, tensile stress, ultimate strain, and strain energy density [63]. However, the two most common methods employed are bone-ligament-bone complexes and isolated ligament samples; although a few other techniques will be mentioned (Figure 2-7).

Bone-ligament-bone complexes consist of a ligament which remains attached to its bony insertion sites. Customized clamps hold each bone in place in a traditional tensile test setup and measures the uniaxial properties of the complex along the collagen direction. The geometries of bone-ligament-bone complexes are typically nonuniform; consequently the setup is highly depend on the alignment of the setup and maintaining anatomical orientation is essential [49]. Studies have reported the slight variation in the orientation and angle of the bones and ligaments induces a significant amount of error [68]. Likewise, this apparatus measures the overall mechanics of the joint system, consequently the measurements are stiffer and higher forces are required. Consequently, failures often occur near the insertion site, which indicates the properties of the insertion sites are being measured instead of the mechanics of the ligament at higher forces. However, this setup is more capable of replicating the mechanical conditions experienced inside the body [69].

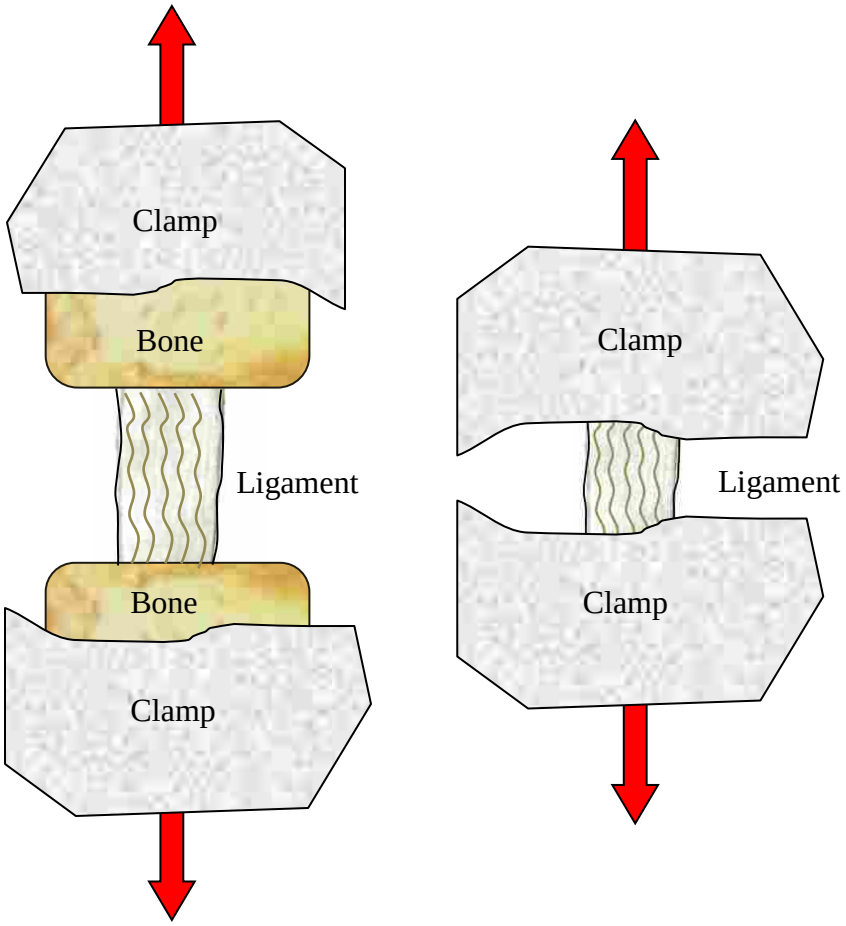

Figure 2-6 Diagram of a (left) bone-ligament-bone setup and a (right) isolated ligament

Testing of isolated ligament samples offers a direct measurement of ligament properties, similar to traditional material testing techniques used in metals and polymers. However, as mentioned earlier, the challenges associated with testing ligaments can introduce several experimental difficulties [52]. Since ligaments are prone to slip in standard tensile testing, the ends of testing samples are typically dried or frozen to achieve full contact [59]. Likewise when ligaments are tested in isolation they are often cut to a bone dog shape. This shape helps to reduce the irregularities in geometry and theoretically provide a well-defined gauge geometry for the sample [49]. Likewise if adequate volume remains in a sample, anisotropic properties can be obtained by using a second test sample oriented perpendicular to the fiber direction. Quapp and

Weiss (1998) used this technique to characterize the anisotropic constitutive response of the medial collateral ligament [43]. Moore employed this methodology and found significant differences in the modulus and ultimate had significant differences ($p < 0.05$) between the transverse and longitudinal samples for the axillary pouch [70].

An additional option for testing the material properties of ligaments is through biaxial testing using sutures. This method sews sutures into the edge of ligaments and pulls the sample in all directions acquiring biaxial data. This method can be tedious in preparation and is also highly dependent on the boundary conditions, which greatly vary between research groups. Suture location along the edge of the test sample must be consistent so uniform boundary conditions are applied [71].

2.5 Biomaterial Characterization

There is a distinct difference between measuring the mechanical response (e.g., force-displacement response) of a system and in characterizing the material constitutive response. Both measurements can be useful, however by characterizing the material constitutive response, engineers can account for geometric changes in the system due to injury, surgery, and remodeling. In order to usefully convey nonlinear, anisotropic, viscoelastic material response data, an accurate constitutive material model is required. Numerous numerical models have advanced the understanding of soft tissues contributions to the overall mechanical response of a joint. This information is essential to understanding the mechanics of injuries and healing of soft tissues [37].

2.5.1 Ligament Material Models

Two types of material models exist: phenomenological and structural [52]. Phenomenological models replicate experimentally measured material behavior without reference to the structural components in a material. Structural models are formulated based on the individual behavior of microstructural components and their interactions. Structural models also allow the correlation of material properties to observed microstructure. Models can further be classified by the types of material behaviors they replicate. Early ligament models neglected time-dependent components and focused primarily on describing the nonlinear elastic aspects of the stress-strain curve, however over the past fifty years viscoelasticity has become a prevalent focus [72].

Elastic models primarily replicate the progressive recruitment of collagen fibers. They assume viscoelastic effects can be ignored. Common material models within this category used to represent ligaments include the piecewise linear elastic model, transversely isotropic elastic models, and the Mooney-Rivlin hyperelastic model [52]. Viscoelastic models have application to variable-rate loading or impact scenarios, and often are structurally based [72]. Quasilinear viscoelastic theory was developed by Fung (1968), and is commonly used to represent all types of soft tissue, including ligaments.

2.5.2 Weiss Constitutive Model

The Weiss model, is a structurally motivated constitutive model capable of characterizing nonlinear anisotropic properties of ligaments, tendons, and fascia; with provisions for viscous relaxation [52, 55, 57]. There are a total of six constitutive parameters (C_1, C_2, C_3, C_4, C_5, λ^*) which represent the microstructural constituents of the biological sample. The strain

energy formulation of the model is shown below in Equation (2-1). The first two terms characterize the constitutive response of the ground substance matrix. F, characterizes the constitutive response of the collagen fibers. The final term accounts for volumetric changes in the tissue. Under physiologic conditions, incompressibility is usually assumed, allowing this term to be neglected [73].

$$W = C_1\ I_1 - 3\ + C_2\ I_2 - 3\ + F\ \lambda\ + \frac{1}{2}K[\ln J\ ]^2 \tag{2-1}$$

The ground substance matrix is modeled using an isotropic hyperelastic formulation. based on the standard deviatoric invariants (I_1 and I_2) of the right Cauchy Green deformation tensor [74]. The response is analogous to a Mooney Rivlin ($C_2 \neq 0$) or Neo-Hookean model ($C_2=0$) [75]. The fiber term, F, is a piecewise continuous function of fiber stretch (λ), representing the behavior of the crimped collagen fibers, as shown in Equation (2-2).

$$\frac{\partial F}{\partial \lambda} = \begin{cases} 0 & \lambda < 1 \\ \frac{C_3}{\lambda}\ \exp\ C_4\ \lambda - 1\ \ - 1 & \lambda < \lambda^* \\ \frac{1}{\lambda}\ C_5\lambda + C_6 & \lambda \geq \lambda^* \end{cases} \tag{2-2}$$

When $\lambda < 1$ the model is isotropic and unable to resist compression. An exponential function describes the straightening of the crimp pattern, where $1 \leq \lambda < \lambda^*$. Here C_3 and C_4 provide a nonlinear characterization of the collagen fiber uncrimping along the fiber direction. Once the critical level λ^* is reached collagen fibers are fully uncrimped and the fiber stiffness increases dramatically. For $\lambda \geq \lambda^*$ a linear equation describes the strain energy contribution of the fibers. C_5 characterizes the linear stiffness of the collagen fibers and C_6 is a dependent term which ensures stress continuity (Equation 2-3). [73]

$$C_6 = C_3\ \exp\ C_4\ \lambda^* - 1\ \ - 1\ - C_5\lambda^* \tag{2-3}$$

The model includes viscoelastic effects through convolution of the Piola-Kirchhoff stress, S(C,t) with a relaxation function *G(t)* (Equation 2-4)

$$S\ C,t\ = S^{e}\ C\ +\ \int_{0}^{t} 2G(t-s)\frac{\delta W}{\delta C(s)}\,ds \qquad (2\text{-}4)$$

Numerically, stress relaxation in the model is typically implemented through a Prony series, as shown in Equation (2-5).

$$G\ t\ =\ \sum_{i=1}^{6} S_i \exp\ \frac{t}{T_i} \qquad (2\text{-}5)$$

2.5.3 Implementation into Finite Element Modeling

The constitutive model developed by Weiss is available in various finite element (FE) packages (FEBio, LS-DYNA, and ABAQUS) for general purpose modeling of transversely isotropic biological materials. The model has been implemented for both volumetric elements (brick, tetrahedral) and shell elements (quadrilateral, triangular), in both implicit and explicit implementations. Several studies have since been conducted validating the application of this model [57, 75-76]

2.6 Interspinous Ligament

Notable findings by previous researchers with respect to the ISL are summarized below in four main topic areas: anatomy, roles, pathology, and material properties.

2.6.1 Anatomy

The ISL inserts posteriorly between adjacent spinous processes at each vertebral joint. The ISL integrates with the SSL and LF on the ventral and dorsal surfaces respectively. Several studies have reported intricate functions of the ISL and SSL, specifically in resisting flexion.

Like other ligaments the ISL is composed of a matrix of collagen fibers, elastin, extracellular matrix, fibroblasts, proteoglycans, water and other proteins [12, 16]. A high amount of elastin is found near the insertion into the LF [12] and dense innervation is found near the insertion of the SSL [77]. The body of the ISL is generally a faded pink, suggesting the ligament is more vascular than other spinal ligaments, which are almost avascular.

One of the most distinctive anatomical features of the ISL is the sigmoidal orientation of the collagen fibers in the mid-section of the structure. Conflicting reports on the orientation of collagen fibers has led to several interpretations of the function of the ISL and several fiber arrangements [10, 16, 19, 78-80] have been proposed. However the majority of these studies report posterior-cranial orientations with a signature sigmoidal curvature in the middle section of the structure [10, 78-80]. This sigmoidal orientation is consistent with our findings and is reported most fully by Scapinelli *et al* (2006). As shown in Figure 2-3 Scapinelli *et al.* characterized the fiber arrangement of the ISL as three distinctive sections: the ventral, middle, and dorsal; where the middle section exhibits a characteristic sigmoidal shape and the exterior sections are predominately oriented obliquely.

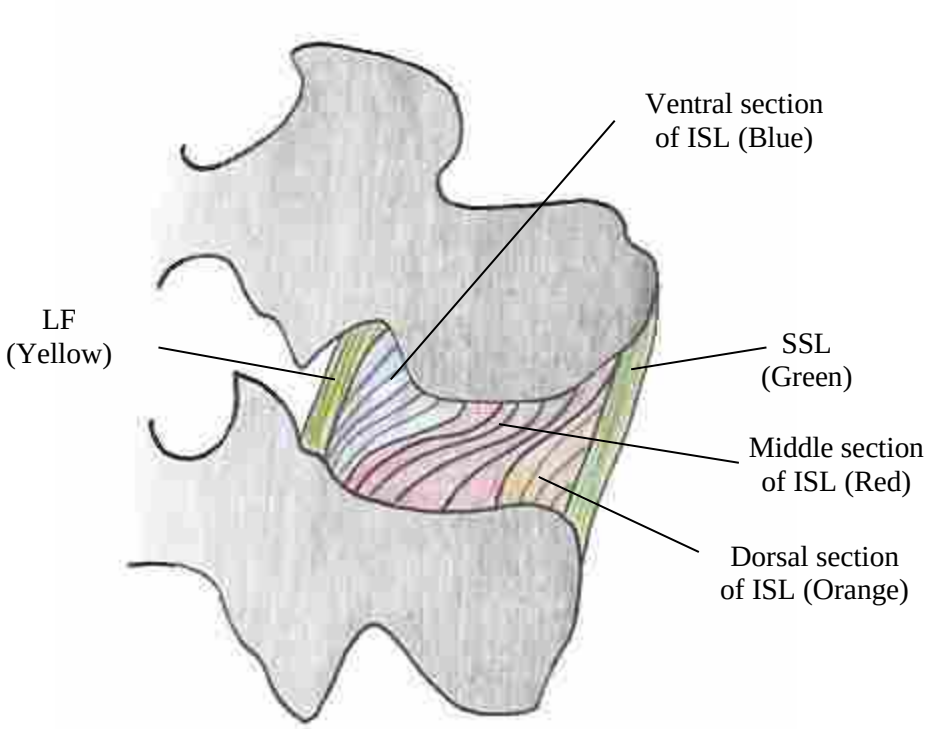

Figure 2-7 Hand-drawn sketch of ISL anatomy illustrating the three sections of the ISL as described by Scapinelli and the surrounding ligaments (LF and SSL)

The study also attributed the unique response of the ISL, in flexion, to incremental recruitment of the constituents of the ISL as shown in Figure 2-9. Thus the unique response of the ISL is not only due to the unique collagen orientation but also the incremental loading of collagen fibers in these three sections. Additional studies have also measured mechanical interactions between collagen fibers of the ISL and interactions among the SSL and LF [12, 24-25].

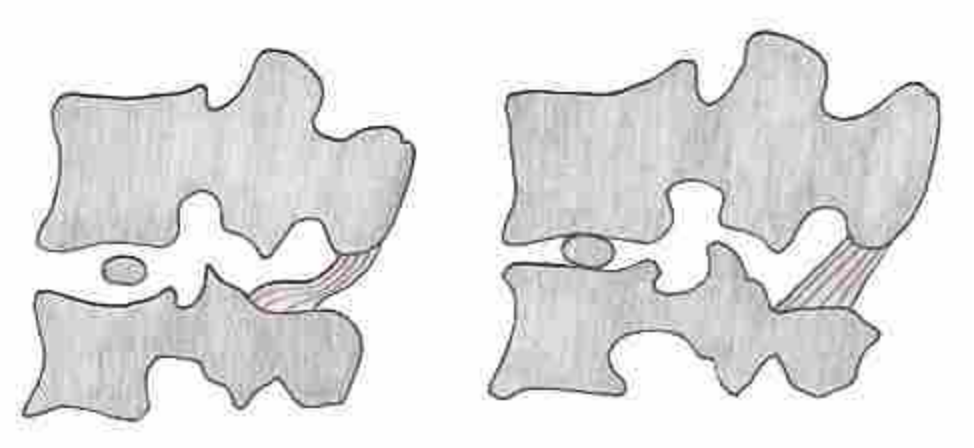

Figure 2-8 Sketch of the incremental recruitment pathway of the ISL

2.6.2 Roles

The ISL has been reported to have vital functions both mechanically and neurologically [25]. However, there also exists a great deal of disagreement in the magnitude of mechanical stability it provides. Some report the ISL to support 75% of the load in the ISL-SSL complex [25] while others report the ISL to have very little functionality [24]. However, most studies agree that the main role of the ISL is to act as a tension-resistant structure in flexion [25, 81]. Likewise the ISL fulfills the typical mechanical roles exhibited by ligaments in the body, previously discussed. Moreover, the ISL-SSL complex has been recognized to provide significant stability to the spinal column, as a complex [82-83]. Neurologically it has mechanoreceptors that are sensitive to strain and cause pain when they are subject to excess strain [84-87]. These embedded mechanoreceptors are believed to provide proprioceptive feedback that inhibits hyperflexion by activating paraspinal muscle contraction [38-39]. Several studies have confirmed spinal ligaments mechanoreceptors are responsive to mechanical strain, serving as nociceptors in lower back pain [34, 85].

2.6.3 Pathology

Midsectional ruptures of the ISL have been reported in up to 21% of subjects over the age of twenty [10]. Rupturing of the ISL has been correlated with age [10, 81], disc herniation [10-11] and disc degeneration ISL segments [83, 88-89]. The ISL also tends to be cut in some surgical procedures, which has been reported to alter the mechanics of the spine. [13] Current clinical devices which influence the ISL function and anatomy include an artificial ISL ligament [90] and interspinous devices [91-93]. Recent studies likewise link the instability of the spine related to ISL degeneration, captured via magnetic resonance imaging [9, 83]. Disruption of the ISL increases spinal motion and induces alternative loading patterns to adjacent spinal components (ligaments, intervertebral disc and musculature), potentially causing additional chronic pain. Histological studies of degenerated ligaments demonstrate local metaplasia [12], ossification [81], and active tissue remodeling [10-11].

2.6.4 Material Properties

Previously reported testing of the biomechanical properties of the ISL has most commonly employed a uniaxial bone-ligament-bone complex testing methodology and reported the measured properties from a total average of the tested cadaveric spinal segments [69, 94]. Studies on the biomechanical properties of the ISL have reported modulus of elasticity, stiffness, average force-deflection curves, and force at failure (Table-1).

However, the nonlinear anisotropic material properties of the ISL have yet to be reported; consequently its mechanical roles remain unclear. This ambiguity is largely attributed to the inability of traditional tensile methods to test the ISL because of its small size and slippery

composition. Furthermore, the inherent nonlinear anisotropic material properties of the ISL are difficult to characterization.

Table 1 Summary of the properties and studies on the ISL

Year	Investigator	Fiber length (mm)	Cross sectional area (mm^2)	Complex
1992	Pintar *et al.*	6.7-30.0	13.8-60	ISL
1982	Panjabi *et al.*	9.6-14.6	none	ISL
1988	Myklebust *et al.*	none	none	ISL
1973	Waters and Morris	none	none	ISL/SSL
1980	Adams *et al.*	7.4-39	1.03-3.5	ISL/SSL
1985	Chazal *et al.*	8.0-14.0	8.0-55.0	ISL/SSL

While these studies provide valuable insight, there is significant ambiguity regarding the mechanical role of the ISL in spinal motion and stability. The reported differences in uniaxial material properties likely arises from variations which naturally occur in biological tissues due to tissue remodeling, degeneration, ossification, injury, or specimen location. Furthermore others have reported challenges defining and isolating the ISL and variations in experimental procedures/objectives often results in conflicting conclusions. Hence, there is a strong need for the present work in characterizing the nonlinear, anisotropic material constitutive response of the ISL.

3 INTERSPINOUS LIGAMENT CHARACTERIZATION

3.1 Introduction

The human interspinous ligament consists of fibrous connective tissue which adjoins the spinous processes of neighboring vertebra. Collectively with other spinal ligaments it creates a passive stability complex which protects the spinal column, specifically in flexion. The nonlinear anisotropic material constitutive properties of the ISL have yet to be reported; consequently the extent of its mechanical role in spinal stability and the consequences for surgical resection remain unclear. The present work utilized anisotropic small punch testing to obtain the material constitutive parameters of the ISL. A total of fifty-six test samples were tested from sixteen ISL specimens. The nonlinear, anisotropic constitutive parameters reported for the ISL are suitable for use in numerical modeling of the lumbar spine.

3.1.1 Anatomy

The human interspinous ligament (ISL) inserts posteriorly between adjacent spinous processes, at each vertebral joint, with ligamentous insertions into the ligamentum flavum (LF) and supraspinous ligament (SSL). Like all ligaments, the ISL is composed primarily of collagen fibers surrounded by an extracellular ground substance matrix [10, 12, 16, 78]. The ISL is notably thicker in the lumbar spine, reflecting a more substantial mechanical role in that region. The body of the ligament is supported by an intricate vascular network [10, 78, 86], reinforced

with elastin in the ventral region [11-12, 16, 78], and densely innervated in the dorsal region [77-78, 86]. Researchers have identified mechanical and neurological roles of the ISL in spinal stability [14, 25], motion control [24, 95], pain transmission [77, 85], and potential parasympathetic action [1, 86].

The ISL is engaged mechanically in the later stages of flexion, acting as a tension resistant structure [11, 22, 25, 78, 80, 94, 96]. The posterior spinal ligament complex—composed of the ISL and SSL—has been recognized to contribute significant stability to the spinal column [82-83]. Moreover, studies of the interdependent nature of the posterior ligament complex report nonuniform loading patterns between the ligaments, where the ISL supports the majority of the load [12, 19, 25].

The unique architecture of the ISL provides a complex in situ mechanical response. The ISL has a posterior-cranial fiber orientation, with a signature sigmoidal curvature in the middle section of the structure [10, 78-80]. The ISL is incrementally recruited during flexion. First the dorsal fibers of the structure close to the SSL are engaged, followed by progressive recruitment of the ventral regions closer to the LF, and finally enlistment of the sigmoidal shaped mid-section [10, 78]. Microscopic interactions among surrounding collagen fibers have also been observed, suggesting that a networking mechanism exists throughout the structure [25].

Substantial evidence demonstrates that failure of the ISL is related to pathologic biomechanics of the spine. Injury to the ISL has been correlated with vertebral instability [9, 83], disc herniation [11, 78], spinal rigidity [10, 81], and muscle dysfunction [1]. Waters and Morris (1973) suggest that idiopathic scoliosis may be related to poor material properties of the ISL–SSL complex [97]. Several investigators have reported that mechanoreceptors within the ISL function as nociceptors in response to excess strain [84-87]. Magnetic resonance imaging studies

have linked degenerative ISL segments to spinal instability [83, 89], disc degeneration [9, 83], facet joint osteoarthritis [83], and Baastrup's disease [98-99]. Histological studies of degenerated ligaments demonstrate local metaplasia [12], sclerosis [100], ossification [81], and active tissue remodeling [10-11].

3.1.2 Biomechanical Properties

There has been substantial work in characterizing the uniaxial mechanical response and morphology of the ISL. Biomechanical properties of the ISL found in literature include: fiber length (6.7-20.0 mm), cross-sectional area (13.8-60.0 mm^2), force at failure (92-185 N), failure stress (1.8-5.9 MPa), failure strain (52.9-119.7%), stiffness (8.7-16.3 N/mm), energy to failure (0.59-2.65 J), and force-deflection curves [69, 94]. Panjabi *et al.*, measured ligamentous strain in spinal segments during flexion-extension, lateral bending and axial rotation. They reported that the ISL and SSL experience the highest failure deformation among spinal ligaments, specifically in flexion [95]. Chazal *et al.*, reported the stress-strain response of the ISL-SSL complex at three characteristic inflection points [22]. Myklebust *et al.* (1988) reported the force and deformation for the ISL at failure through the entire spinal column, finding that the strongest ligaments were in the cervical and lumbar regions [94]. Pintar *et al.* (1992) correlated force-deflection curves previously measured by Myklebust with geometrical measurements from independent cadavers to determine averages of stress, strain, stiffness, and energy to failure for each level of the lumbar region [69].

These studies have established both geometric properties and failure criteria for the ISL. However, the nonlinear anisotropic material properties of ISL prior to failure have yet to be reported. Consequently, the ISL is typically represented by hyperelastic line elements in numerical models of the spine (e.g., FE models [101-102]). Line elements can accurately convey

simple tension, but do not accurately represent shear response, coupled ligament insertions, nor the sigmoidal collagen architecture of the midsubstance ISL. Line elements are theoretically capable of providing an incremental recruitment similar to that seen in the ISL, but due to the complexity and uncertainty associated with manually assigning this behavior to individual line elements, no models to date have done so. A three dimensional anisotropic continuum representation of the ISL is necessary to accurately portray the complex loading conditions present at the ISL's ligamentous and bony insertions. Thus, the objective of the present work was to characterize the nonlinear, anisotropic constitutive properties of the ISL.

3.2 Methods

3.2.1 Dissection & Sample Preparation

Six cadaveric spines (demographic information may be found in Table 1) were obtained through an accredited tissue bank following an IRB approved protocol. None of the spines had a history of spinal disorders or spinal surgery and no obvious abnormalities. Surrounding muscle, fascia, and subcutaneous tissues were carefully resected on the posterior surface of each spine to locate the ISL. The ISL was then removed by making incremental incisions along the bony and ligamentous insertions sites. Upon removal each ISL specimen was individually wrapped in saline soaked gauze, vacuum sealed, flash frozen (PELCO Histo/Cyto-Freeze, Ted Pella Inc., Redding), and stored in a -25º C freezer until testing. Hydration was maintained throughout dissection and testing by spritzing the tissue with a saline solution.

Table 2 Summary of the demographic information for each cadaveric specimen used in testing

Spine ID	Sex	Age	Weight (lbs)	Height (ft)
A	F	47	250	4.92
B	F	56	130	5.08
C	F	79	81	5.24
D	F	86	140	5.33
E	M	50	80	5.83
F	M	67	115	5.64

Prior to testing ISL specimens were individually removed from the freezer and thawed to room temperature in preparation for testing. Each ISL specimen was then sectioned with a microtome blade into multiple test samples per ISL specimen (see Figure 1). First, the specimen was sliced through the midsagittal plane (dorsal to ventral), dividing the ISL into mirrored halves of comparable thickness. Subsequently, if adequate material remained, each half was sectioned again (superior to inferior), such that each test sample was approximately 6mm x 6mm x 0.5mm in dimension. The location, anatomical integrity, and fiber orientation of each test sample was recorded.

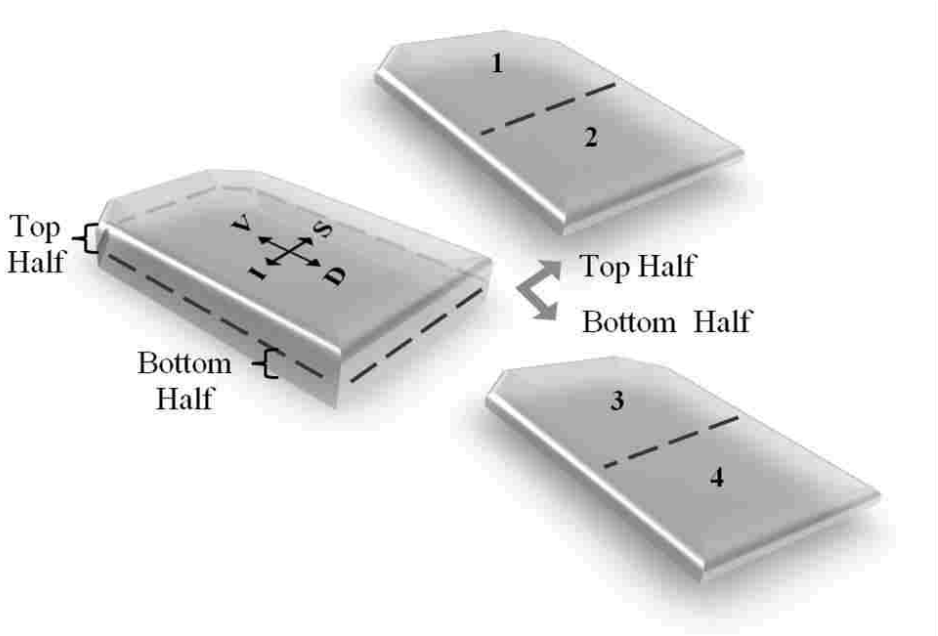

Figure 3-1 Illustration of ISL sectioning procedure (left) initial sectioning of the specimen into equal mirrored halves (right) sectioning of halves into additional samples (Where S = superior, I = inferior, V = ventral, D = dorsal)

3.2.2 Testing Methodology

The Anisotropic Small Punch Tester (ASPT) is a testing device capable of accurately measuring the nonlinear anisotropic properties of ligaments [103-104]. The primary components, shown in Figure 2, consist of an optical system, and data collection system. The optical system consisted of two orthogonally placed CCD cameras (scA640-70fm, Basler Vision Technologies, Germany) mounted with macro zoom lenses (MLH-10X, Computar, New York) located in the plane of action, and a superiorly placed microscope (CM1-USB microscope). The cameras captured the samples displacement profiles of in the longitudinal (parallel to fiber direction) and transverse (perpendicular to fiber direction) directions. The microscope recorded topological image data to verify that no localized slipping occurred at the clamp/sample interface during the testing process. Force-deflection data was measured by a 22 lbs load cell and linear potentiometer, which were both mounted inferior to the apparatus. Synchronized data acquisition

from the optical and mechanical measuring systems was obtained using a custom Labview program (Labview, version 9.0, National Instruments, Austin).

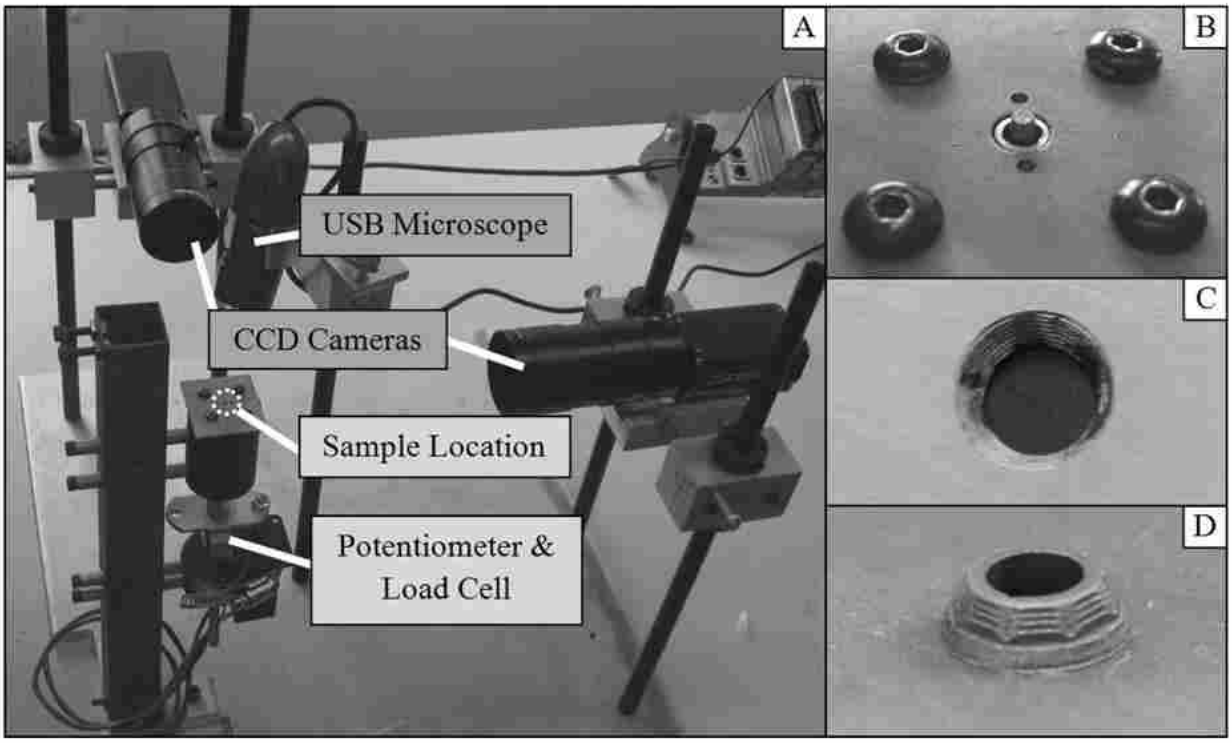

Figure 3-2 (A) Diagram of the ASPT setup. Images B-D show zoomed images of testing the apparatus. (B) Punch rod and clamping screws (C) top plate grip surface (D) bottom grip surface. Texturing on the clamping surfaces of the ASPT provided additional sample fixation and reduced the required clamping force (C-D).

The thickness of each test sample was measured and confirmed to have a consistent cross section via the calibrated ASPT optical systems. Prior to testing, each sample was aligned along the predominant collagen direction, such that the longitudinal and transverse responses were captured by the two orthogonal CCD cameras. The sample was preconditioned to negate viscoelastic effects by vertically displacing the 1.8 mm diameter punch rod at a rate of 0.2 mm/second for 10 cycles. The load cell and potentiometer were then recalibrated. Finally, the sample was tested by displacing the punch rod at a rate of 2 mm/second until sample failure.

Punch force and deflection were measured respectively via the 22 lbs load cell and potentiometer with accuracies of ± 0.005 lbs and ± 0.01 mm.

3.2.3 Material Characterization

The material response of the ISL was modeled using a nonlinear, anisotropic constitutive model first proposed by Weiss *et al.* [43, 57]. The Weiss model has previously been used to characterize the medial collateral ligament of the knee, glenohumeral capsule of the shoulder, and interosseous ligament of the forearm [70, 105-106]. The model consists of six constitutive parameters—C_1, C_2, C_3, C_4, C_5 and λ^*—which represent the mechanical response of the microstructural components of ligaments. Specifically the ground substance matrix is represented by C_1 and C_2 and the collagen fibers are represented by the remaining parameters C_3, C_4, C_5, and λ^*. The ground substance matrix is defined as a Mooney-Rivlin model (when $C_2 \neq 0$) or Neo-Hookean model (when $C_2 = 0$). The parameters C_3 and C_4 are coupled, and correspond to the measured material response during collagen fiber uncrimping, C_5 is the tangent modulus after the fibers are uncrimped, and λ^* is the stretch at which the collagen fibers are uncrimped.

A FE model corresponding to the geometry, boundary conditions, and loading scenario of each ASPT test sample was generated. The FE model and associated experimental force-deflection values were then input into a system identification optimization routine. The objective of the optimization routine was to minimize the mean square error between the experimental force-deflection profile and the force-deflection profile generated by the FE model. This was accomplished by varying the constitutive material parameters of the FE model using a leapfrog simulated annealing approach. The optimization routine was terminated after 20 iterations or when the incremental change in the objective function was reduced to 0.005% between iterations.

3.3 Results

A total of fifty-six test samples were collected from sixteen ISL specimens, removed from six thoracolumbar cadaveric spines. The number of test samples, per ISL specimen, varied from 1 to 6 averaging a total of 3 ± 2 tests per specimen. The average force stress at failure occurred at 8.3 ± 4.8 MPa while the strain at failure was 71.1 ± 31.4 %. When viewing the optical data 14 test samples were identified to either slip (n=4) or tear (n=10) at the grips. The constitutive parameters of the remaining thirty-nine test samples were obtained as described above. The average coefficient of determination (R^2) of the experimental and FE force-displacement results as predicted by the material constitutive response was 0.984. A summary of the constitutive parameters (C_1, C_3, C_4, C_5, λ^*) determined by the system optimization procedure is shown in Table 2. Table 3 and Table 4 display the constitutive parameters as average values, grouped by a functional spinal level or cadaveric identification. The tables also report test sample thickness (t), and the number of test samples (n) in each grouping.

Table 3 Results summary of material parameters obtained for all ISL test samples

	C_1	C_3	C_4	C_5	λ^*	R^2	t (mm)
Mean	0.27	0.62	13.27	20.08	1.09	0.984	1.02
S.D.	0.14	0.57	10.06	13.62	0.04	0.021	0.39
Max	0.50	2.00	35.00	45.00	1.17	0.999	2.14
Min	0.04	0.01	1.10	3.00	1.01	0.906	0.33

Table 4 Average values for ISL material parameters, differentiated by the functional spinal level

Level	n	C_1	C_3	C_4	C_5	λ*	R^2	t (mm)
T10-T11	3	0.20 (0.20)	1.09 (0.39)	17.20 (2.31)	32.35 (6.94)	1.097 (0.007)	0.998 (0.003)	0.81 (0.08)
T11-T12	6	0.30 (0.09)	0.70 (0.73)	15.49 (10.14)	31.22 (10.03)	1.115 (0.042)	0.993 (0.007)	0.88 (0.20)
T12-L1	4	0.34 (0.12)	0.32 (0.26)	21.07 (17.33)	25.71 (17.83)	1.085 (0.015)	0.986 (0.012)	0.91 (0.39)
L1-L2	8	0.24 (0.00)	0.53 (0.10)	14.70 (8.85)	16.65 (7.22)	1.074 (0.008)	0.980 (0.012)	1.03 (0.01)
L2-L3	12	0.27 (0.06)	0.52 (0.33)	14.34 (10.68)	18.98 (11.17)	1.085 (0.006)	0.986 (0.012)	1.17 (0.21)
L3-L4	5	0.24 (0.08)	0.53 (0.73)	8.42 (0.22)	8.74 (2.51)	1.089 (0.016)	0.982 (0.002)	1.01 (0.56)
L4-L5	4	0.27 (0.13)	0.46 (0.20)	8.22 (11.93)	9.37 (4.26)	1.078 (0.045)	0.973 (0.039)	0.91 (0.47)

Table 5 Average values for ISL material parameters, based on cadaveric identification

ID	n	C1	C3	C4	C5	λ*	R^2	t (mm)
A	2	0.31 (0.17)	0.14 (0.06)	15.55 (20.44)	20.27 (14.74)	1.090 (0.014)	0.994 (0.002)	1.34 (0.02)
B	13	0.30 (0.14)	0.41 (0.48)	16.93 (11.21)	22.18 (14.73)	1.078 (0.029)	0.976 (0.027)	0.95 (0.48)
C	4	0.28 (0.18)	0.49 (0.94)	9.74 (3.05)	12.84 (7.76)	1.095 (0.015)	0.987 (0.008)	0.98 (0.40)
D	5	0.33 (0.09)	0.54 (0.43)	11.23 (12.05)	16.74 (15.49)	1.085 (0.060)	0.979 (0.014)	0.95 (0.21)
E	4	0.24 (0.05)	0.69 (0.88)	22.24 (9.44)	38.98 (11.75)	1.110 (0.040)	0.995 (0.002)	0.69 (0.10)
F	14	0.22 (0.15)	0.80 (0.51)	13.74 (9.95)	15.94 (12.01)	1.083 (0.031)	0.986 (0.023)	1.04 (0.43)
TOTAL	42	0.27 (0.14)	0.61 (0.57)	13.22 (10.18)	20.16 (13.78)	1.087 (0.036)	0.984 (0.021)	1.03 (0.40)

3.4 Discussion

Where possible, the material parameters were compared with previously reported uniaxial biomechanical properties. C_5 is a measurement of the post-uncrimping stiffness of the ligament along the fiber direction, thus it can be related to the total stiffness values reported by other researchers. Stiffness values (N/mm) previously reported for the ISL can only be compared to equivalent units of C_5 (MPa), when the values for ligament length and cross-sectional area are provided. Unfortunately the majority of literature reporting the ISL material response was obtained by testing the SSL-ISL complex [22-23] or do not report sample cross-sectional area [94-95]. For example, the average stress (8.71 ± 3.05 MPa) and strain (0.39 ± 0.15%) were reported at failure by Chazal *et al.* for the ISL-SSL complex [22]. These stress values are within one standard deviation of the stress values obtained from the ASPT. However, the strain measured in the ASPT is significantly greater than what Chazal reported for the ISL-SSL complex, which is to be expected since the SSL provides additional fiber recruitment. Stiffness values reported by Pintar *et al.* were compared with C_5 by multiplying the reported stiffness by the ratio of the original length to cross-sectional area [69]. The resulting comparison is shown in the first two columns of Table 5. Standard deviations for this data could not be calculated, since the number of test samples was not reported. Pintar *et al.* also reported stiffness, stress at failure, and strain at failure based on spinal level, which is shown in the remaining columns of Table 5 for comparison to the ASPT values. There is generally good agreement between the two data sets, although it should be noted that the "total stiffness" reported by Pintar does not subtract the fiber strain prior to uncrimping and thus will generally be lower than C_5.

Table 6 Comparison of stiffness and stress and strain values at failure collected from the ASPT and compared to results published by Pintar *et al.* [69]

	Stiffness (Mpa)		Stress at Failure (Mpa)		Strain at Failure (%)	
	ASPT	Pintar	ASPT	Pintar	ASPT	Pintar
T10-T11	32.4 ± 14.3	--	12.8 ± 6.7	--	54.1 ± 21.3	--
T11-T12	31.2 ± 10.0	--	10.9 ± 4.4	--	55.9 ± 15.4	--
T12-L1	27.4 ± 24.9	12.1	12.9 ± 3.0	4.2 ± 0.2	122.9 ± 107.9	59.4 ± 36.1
L1-L2	17.9 ± 14.5	10	7.9 ± 5.1	5.9 ± 1.8	76.2 ± 30.9	119.7 ± 14.7
L2-L3	19.2 ± 11.7	9.6	8.0 ± 4.4	1.8 ± 0.1	67.2 ± 19.2	51.5 ± 2.9
L3-L4	9.8 ± 4.8	18.1	4.5 ± 1.9	1.8 ± 0.3	80.9 ± 28.7	96.5 ± 35.8
L4-L5	9.4 ± 4.3	8.7	4.7 ± 1.3	2.9 ± 1.9	83.0 ± 19.1	87.4 ± 6.9
Total	20.1 ± 13.6	11.5	8.3 ± 4.7	--	71.0 ± 31.1	--

The Weiss constitutive model has been implemented into several commercial and research FE software packages (e.g., LS-DYNA, ABAQUS, FEBio) facilitating the implementation of the present work into computational spine models. However, other material models are capable of accurately characterizing the nonlinear, anisotropic response of the ISL [52-53, 73, 107]. Ligament pre-strain and stress-relaxation were not included in the present work but are important to the function of ligaments [44, 47, 49, 59]. These characteristics will be obtained in future work.

The fourteen samples that were rejected from the study due to tearing or slipping at the grips were related to two extremes in pathology: calcification and degeneration. Calcified ISL test samples would easily slip when gripping the sample while obviously degenerated ISL samples would tear in the grips within an extremely low force range (9.3±5 N). Since both of these conditions violate the boundary conditions assumed in the FE model and they could not be characterized. Degenerative samples demonstrated low collagen fiber organization and high ground substance content. Ossified ligaments were small in size and difficult to section and grip.

The applied methodologies were found to successfully measure and derive accurate nonlinear anisotropic material properties for the human ISL. The high R^2 values obtained between the experimental results and the optimized material constitutive behavior are attributed to the use of FE models which precisely matched the geometry of the test samples and to the efforts undertaken to minimize experimental error in the ASPT setup. The ability to test multiple samples per ISL specimen provides a mechanism for direct comparison of material properties as a function of spine level and between cadaveric spines. To the authors' knowledge, this is the first study which provides nonlinear, anisotropic material constitutive parameters for the ISL. The listed results provide constitutive parameters that will allow FE spine models to provide more fidelic representations for the ISL using nonlinear anisotropic elements (shell element and volumetric elements) that can more accurately represent shear load transfer.

3.5 Acknowledgements

Funding for this research was provided by the National Science Foundation (CMMI-0952758).

4 ADDITIONAL INSIGHTS

This chapter presents and discusses items which were not included within the technical publication (Chapter 3), due to space constraints. First, observations of the pathology within the ISL are discussed. Next, the material properties found for the ISL are compared to other constitutive parameters obtained for ligaments found in the human body.

4.1 Affects of Averaging Material Properties

Due to the limitations of traditional testing methods, previous studies have obtained the material properties of the ISL by using an cross-population average of the properties measured for each cadaver specimen [19, 22, 69, 94]. However, since the ASPT method provides the opportunity to obtain multiple test samples per specimen, the variation in tangent stiffness (C_5) between spine donors, and among functional spinal levels was investigated. As demonstrated in Figure 4-1 a cross-population average (represented by the black dashed line) does not capture the donor-specific variation in tangent stiffness.. Averaging the total average of the 42 test samples yields a stiffness of 20.08±13.62. The maximum standard deviation was reduced to 9.33 when stiffness properties were organized by donated spine. Note each diamond on the chart represents the average stiffness for each spine respectively.

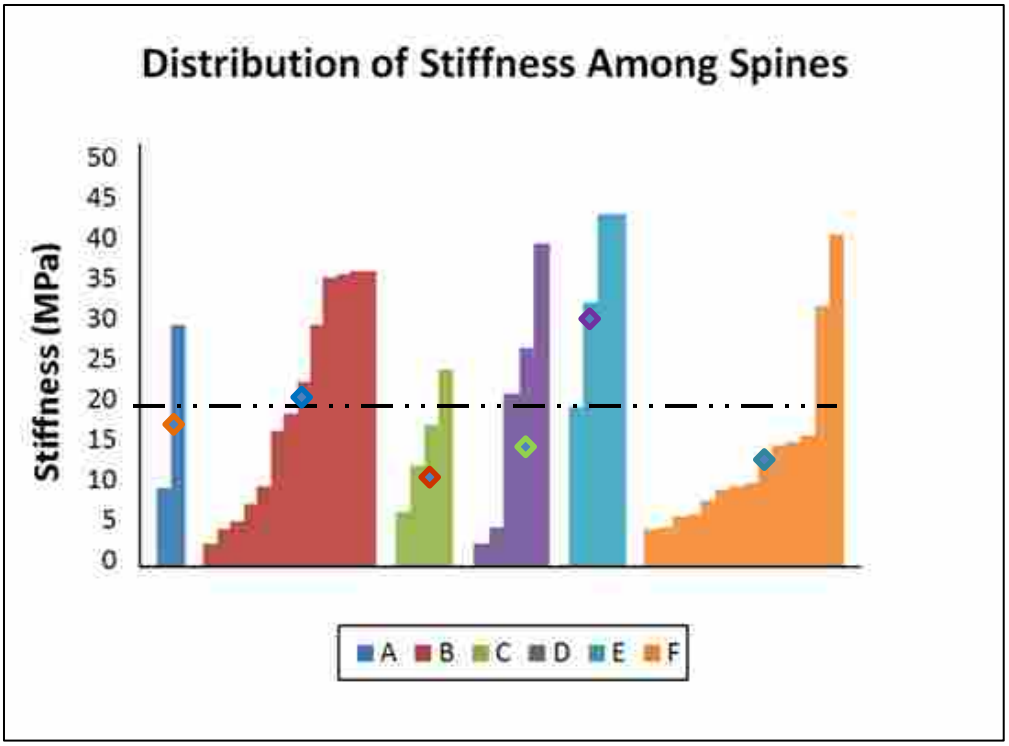

Figure 4-1 Distributions of stiffness (C_5) among the total test samples (n =42). Specimen stiffness is organized from lowest to highest and sorted by spine donor.

Figure 4-2 shows the minimum, average, and maximum values of ISL tangent stiffness as grouped by spine level. In examining this graph one observes a decreasing stiffness as the spinal column descends. This trend is consistent with observations regarding lumbar mobility in both our own lab as well as in journal publications by other research groups. First the lumbar region has been shown to have the highest range of motion compared to the remainder of the spine [108]. Likewise the ligaments of the lumbar region are more susceptible to injury due to the high loads imposed on them. Injured ligaments would demonstrate a lower stiffness [109-111].

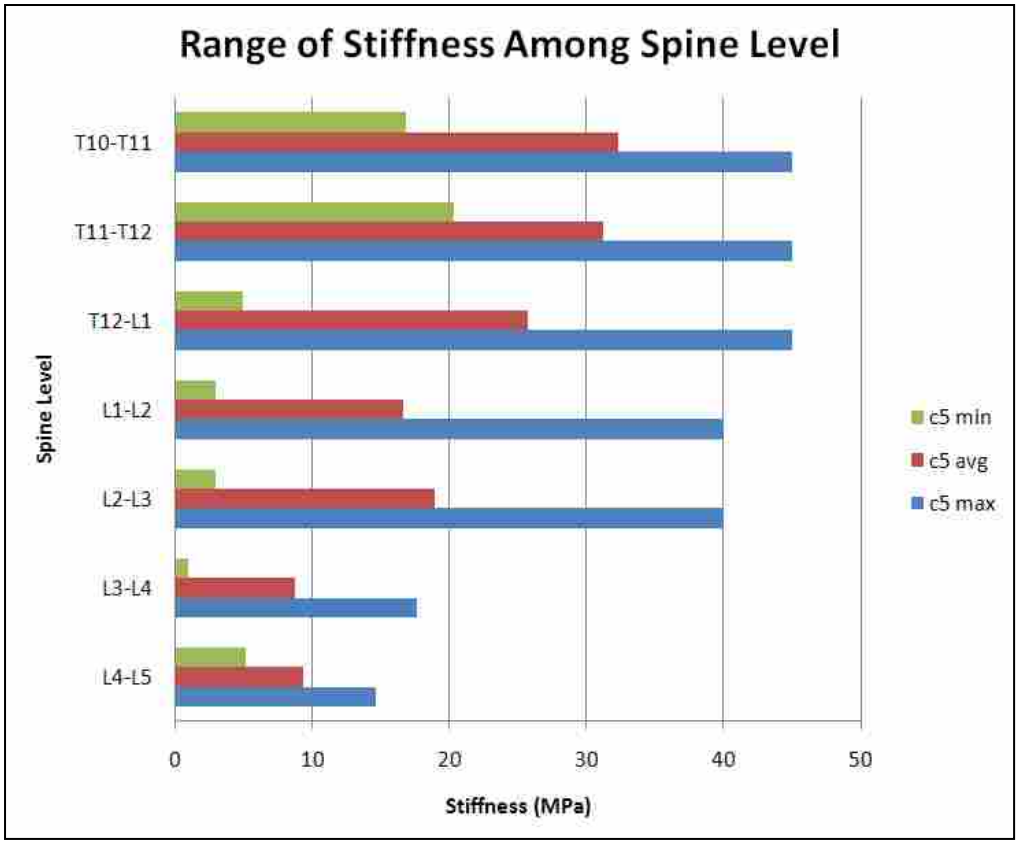

Figure 4-2 Range of stiffness among spine levels

4.2 Material Properties Comparison

The constitutive behavior of the ISL is notably different from that reported for knee, shoulder, and hip ligaments. Specifically, the high collagen fiber content and unique collagen architecture provided a less stiff material response. The total average of the results from the present work is compared below with available data from the literature for the medial collateral ligament (MCL) [43].

Table 7 Table comparing constitutive properties of the ISL to the MCL

	c_1	c_3	c_4	c_5	λ^*
ISL	0.27	0.61	14.77	20.31	1.08
	(0.13)	(0.55)	(11.00)	(13.26)	(0.03)
MCL	1.44	0.57	48.00	457.10	1.06
	(0.33)	(0.02)	(0.36)	(12.50)	(177.40)

4.3 Pathology Associated with the ISL

The small size of the ISL, buried in the dense anatomy of the spine, initially seemed indistinct and difficult to isolate. Several other studies have likewise reported difficulty in distinguishing the ISL from the surrounding anatomy [24-25, 78]. However, with time the team became more experienced with spinal dissection and the isolation of the ISL became significantly easier. Specifically the identification of the spinalis and interspinalis muscles was guided by palpating the spinous processes. These muscles were then carefully resected with a scalpel. The ISL would was consistently deep to this tissue.

One of the most controversial aspects of the ISL found in literature is in regards to the fiber orientation of the ISL. However, the most consistent descriptions which correlate with our observations report a sigmoidal curvature in the mid-section of the ISL and posterior-cranial orientation of the remaining fibers [10, 78-80]. Specifically, a recent study by Scapinelli in 2006, describes the ISL in three distinct regions, to which he referred to as the ventral, middle and dorsal fiber bundles. The ventral section was fused to the LF, inserting posteriorly-inferiorly to the central aspect of the spinous process. The middle section had the largest volume and formed a thick italic S-shaped curve, which was believed to be the main component of resistance to flexion. Lastly, the dorsal section inserted obliquely backwards converging into the SSL. Likewise the degree of tilt of the S-shaped curve varied within samples depending environmental

loading. This report was consistent with observations of our ISL specimens; however we also noted that the sigmoidal shape becomes less prominent in pathological samples.

Throughout the spinal dissections several types of pathologies were identified to be associated with degenerative ISL specimens: calcification, metaplasia, degeneration and rupture. These pathologies presented several challenges to material characterization. First, specimens subject to these identified pathologies were significantly reduced in size. Consequently, it was very difficult to obtain an adequate testing sample for material characterization. Secondly, pathological samples often had very poor composition and were difficult to grip. For example calcified samples were nearly impossible to test, as there composition was comparable to bone. In contrast, samples with degenerative characteristics had very low collagen content and primarily consisted of ground substance matrix. These two extreme types of samples were extremely difficult to grip. Calcified samples and were difficult to section and would easily slip when gripping the sample while degenerative samples would tear in the grips within an extremely low force range (9.3±5 N). Since both of these conditions violate the boundary conditions assumed in the FE model, they could not be characterized using our standard techniques. Consequently, extreme cases of pathological samples were not included in our data set.

Unfortunately, these pathologies could not directly be associated with causation, based on demographic information. However, several studies link the primary origin of degeneration and calcification with aging [12, 112]. This point brings up an additional concern. To our knowledge no method currently exists which classifies the degeneration or calcification of ligaments. One example of a system which rates the degeneration of an intervertebral disc, on a scale of one to five, is the Thompson scale. To demonstrate the value of this type of system a contrast of this

scale is compared to hematoxylin and eosin (H&E) microstructure images taken of the ISL, represented in Figure 4-1. The H&E images were taken for a separate, ongoing study which is correlating the microstructural properties to the material properties measured in this study.

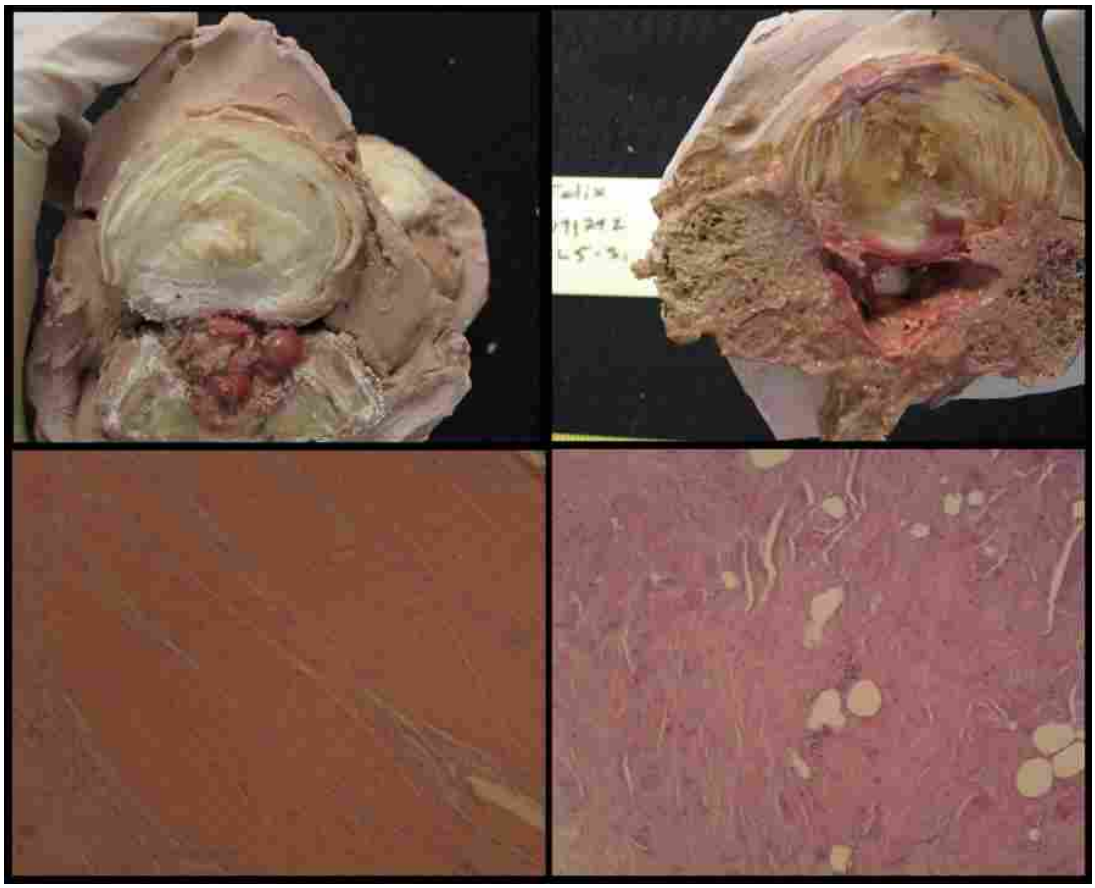

Figure 4-3.Top: Representation of Thompson scale: (Left) Healthy—Grade 1, (Right) Unhealthy—Grade 5, Bottom ISL H & E samples: (Left) Healthy and (Right) Unhealthy

From quick inspection once can see the visual discrepancies that exist in the microstructures of the ISL at different stages of degeneration. We believe that a need exists for grading of pathology associated with the ISL. The pathology of the ISL is underrepresented in the literature and deserves increased attention. A similar system could also correlate to the ligament pathology from other joints, and would clarify the etiology. We also observed that

pathology in the ISL was often associated with pathologies of other spinal tissues; particularly disc degeneration.

5 CONCLUSION

The present work captured the nonlinear anisotropic constitutive response of the ISL for what we believe may be the first time. Material properties were found to vary for each specimen and be dependent on the sample integrity, thickness and location. These findings are anticipated to clarify the properties and roles of the ISL in spinal stability and to provide accurate material properties for finite element spine models. Refinement and development of the tools and techniques associated with the ASPT was a substantial portion of this thesis work and we believe that it has potential to transform the status quo for mechanical testing of biological tissues.

5.1 Directions for Research

The results of this study are part of a continuous effort to understand the roles of spinal ligaments in spinal stability. This research fits in the context of two ongoing efforts. First, a great strength of the BABEL laboratory is FE modeling and it is anticipated these results will be implemented into a subject specific lumbar FE model to support further investigation of spinal ligament mechanics. Secondly, these material properties will be correlated with microstructural parameters taken from the same samples. Consequently, there are several aspects of this research which could be pursued: (1) the material properties of the remaining spinal ligaments (ALL, PLL, FJC, and LF) could be characterized, (2) inclusion of viscoelasticity and pre-strain in material characterization (as available in the Weiss constitutive model), and (3) examination of the variation in mechanical response when different ISL material properties serve as input into

the computational lumbar spine FE model. Finally, throughout this research several additional topics of interest related to the ISL were identified. To clearly present these potential topics they are rhetorically stated.

- What aspects of inhomogeneity in material properties exist in the ISL due to the sigmoidal characteristic?
- How can one qualitatively and quantitatively assess the pathology associated with an ISL sample and what modifications would need to be made to measure its material properties?
- What are the consequences of averaging material properties of soft tissues? How does the ISL affect the mechanical stability of the spine?
- What significance do these results have in relation to numerical models of the spine?
- What is the loading pathway of the ISL and how does it interact with the surrounding spinal tissues?
- What correlations can be found between the mechanical properties and microstructure of the ISL?
- In what ways does the pathology of the ISL contribute to lower back pain?

5.2 Summary of Contributions

This research has been published and presented in several conferences with associated abstracts: Orthopedic Research Society (ORS), Mountain West Bioengineering Conference, and Utah State University (USU) Graduate Research Symposium. A conference paper on the methodology of the ASPT was presented at the annual meeting of the Society of Experimental Mechanics (SEM) and published in the conference proceedings report. A 2nd place award was

obtained for the podium presentation at the USU Graduate Research Symposium. The primary work of this thesis has been submitted for publication in the Journal of Biomechanical Engineering and is currently in review.

The primary contributions of this work include: 1) Characterization of the nonlinear anisotropic material properties of the ISL, which are suitable for application in numerical models of the spine, 2) Development of a novel biomechanical testing method (ASPT) which is transferable to other types of soft tissue testing, and 3) Identification of experimental techniques which assist extracting multiple samples from very small specimens.

REFERENCES

[1] M. M. Panjabi, "A hypothesis of chronic back pain: ligament subfailure injuries lead to muscle control dysfunction," *Eur Spine J,* vol. 15, pp. 668-676, May 2006.

[2] G. M. Franklin, *et al.*, "Outcome of Lumbar Fusion in Washington State Workers' Compensation," *Spine,* vol. 19, pp. 1897-1903, 1994.

[3] M. C. Jensen, *et al.*, "Magnetic resonance imaging of the lumbar spine in people without back pain," *N Engl J Med,* vol. 331, pp. 69-73, Jul 14 1994.

[4] L. M. S. Hashemi, *et al.*, "Length of Disability and Cost of Workers' Compensation Low Back Pain Claims." *J Occup Environ Med,* vol 39, pp. 937-945, Oct 1997

[5] H. R. Guo, *et al.*, "Back pain prevalence in US industry and estimates of lost workdays," *Am J Public Health,* vol. 89, pp. 1029-35, Jul 1999.

[6] J. W. Frymoyer and W. L. Cats-Baril, "An overview of the incidences and costs of low back pain," *Orthop Clin North Am,* vol. 22, pp. 263-71, Apr 1991.

[7] A. Strayer, "Lumbar spine: common pathology and interventions," *J Neurosci Nurs,* vol. 37, pp. 181-93, Aug 2005.

[8] P. O'Leary, *et al.*, "Response of Charite total disc replacement under physiologic loads: prosthesis component motion patterns," *Spine J,* vol. 5, pp. 590-9, Nov-Dec 2005.

[9] A. Fujiwara, *et al.*, "The interspinous ligament of the lumbar spine. Magnetic resonance images and their clinical significance," *Spine (Phila Pa 1976),* vol. 25, pp. 358-363, Feb 1 2000.

[10] P. M. Rissanen, "The surgical anatomy and pathology of the supraspinous and interspinous ligaments of the lumbar spine with special reference to ligament ruptures," *Acta Orthop Scand Suppl,* vol. 46, pp. 1-100, 1960.

[11] H. Yahia, *et al.*, "Degeneration of the human lumbar spine ligaments. An ultrastructural study," *Pathol Res Pract,* vol. 184, pp. 369-375, Apr 1989.

[12] L. H. Yahia, *et al.*, "Ultrastructure of the human interspinous ligament and ligamentum flavum. A preliminary study," *Spine (Phila Pa 1976),* vol. 15, pp. 262-268, Apr 1990.

[13] J. F. Cusick, *et al.*, "Biomechanics of sequential posterior lumbar surgical alterations," *J Neurosurg,* vol. 76, pp. 805-11, May 1992.

[14] A. A. White and M. M. Panjabi, *Clinical Biomechanics of the Spine* vol. 2. Philadephia: Lippincott, 1990.

[15] K. L. Moore and D. A.F., "Clinically Oriented Anatomy," J. Glazer and C. Odyniec, Eds., 5 ed. Baltimore: Lippinocott Williams & Wilkins, 2006, pp. 478-97.

[16] J. F. Behrsin and C. A. Briggs, "Ligaments of the lumbar spine: a review," *Surg Radiol Anat,* vol. 10, pp. 211-219, 1988.

[17] H. Tkaczuk, "Tensile properties of human lumbar longitudinal ligaments," *Acta Orthop Scand,* Suppl 115, 1968.

[18] H. Ohshima, *et al.*, "Morphologic variation of lumbar posterior longitudinal ligament and the modality of disc herniation," *Spine (Phila Pa 1976),* vol. 18, pp. 2408-11, Dec 1993.

[19] D. W. Hukins, *et al.*, "Comparison of structure, mechanical properties, and functions of lumbar spinal ligaments," *Spine (Phila Pa 1976),* vol. 15, pp. 787-795, Aug 1990.

[20] M. C. Kirby, *et al.*, "Structure and mechanical properties of the longitudinal ligaments and ligamentum flavum of the spine," *J Biomed Eng,* vol. 11, pp. 192-6, May 1989.

[21] M. van Kleef, *et al.*, "12. Pain originating from the lumbar facet joints," *Pain Pract,* vol. 10, pp. 459-69, Sep-Oct 2010.

[22] J. Chazal, *et al.*, "Biomechanical properties of spinal ligaments and a histological study of the supraspinal ligament in traction," *J Biomech,* vol. 18, pp. 167-176, 1985.

[23] M. A. Adams, *et al.*, "The resistance to flexion of the lumbar intervertebral joint," *Spine (Phila Pa 1976),* vol. 5, pp. 245-253, May-Jun 1980.

[24] R. J. Hindle, *et al.*, "Mechanical function of the human lumbar interspinous and supraspinous ligaments," *J Biomed Eng,* vol. 12, pp. 340-344, Jul 1990.

[25] J. P. Dickey, *et al.*, "New insight into the mechanics of the lumbar interspinous ligament," *Spine (Phila Pa 1976),* vol. 21, pp. 2720-2727, Dec 1 1996.

[26] J. A. Vilensky, *et al.*, "Serratus posterior muscles: anatomy, clinical relevance, and function," *Clin Anat,* vol. 14, pp. 237-41, Jul 2001.

[27] L. Hansen, *et al.*, "Anatomy and biomechanics of the back muscles in the lumbar spine with reference to biomechanical modeling," *Spine (Phila Pa 1976),* vol. 31, pp. 1888-99, Aug 1 2006.

[28] K. M. Tesh, *et al.*, "The abdominal muscles and vertebral stability," *Spine (Phila Pa 1976),* vol. 12, pp. 501-8, Jun 1987.

[29] J. Garcia-Cosamalon, *et al.*, "Intervertebral disc, sensory nerves and neurotrophins: who is who in discogenic pain?," *J Anat,* vol. 217, pp. 1-15, Jul 2010.

[30] M. A. Edgar, "The nerve supply of the lumbar intervertebral disc," *J Bone Joint Surg Br,* vol. 89, pp. 1135-9, Sep 2007.

[31] L. Yahia, *et al.*, "Sensory innervation of human thoracolumbar fascia. An immunohistochemical study," *Acta Orthop Scand,* vol. 63, pp. 195-7, Apr 1992.

[32] C. H. Rivard, *et al.*, "[Morphological study of the innervation of spinal ligaments in scoliotic patients]," *Ann Chir,* vol. 47, pp. 869-73, 1993.

[33] S. Rhalmi, *et al.*, "Immunohistochemical study of nerves in lumbar spine ligaments," *Spine (Phila Pa 1976),* vol. 18, pp. 264-7, Feb 1993.

[34] N. Bogduk, *et al.*, "The human lumbar dorsal rami," *J Anat,* vol. 134, pp. 383-97, Mar 1982.

[35] P. B. Wu, *et al.*, "The lumbar multifidus muscle in polysegmentally innervated," *Electromyogr Clin Neurophysiol,* vol. 40, pp. 483-5, Dec 2000.

[36] C. B. Frank, "Ligament structure, physiology and function," *J Musculoskelet Neuronal Interact,* vol. 4, pp. 199-201, Jun 2004.

[37] H. J. Jung, *et al.*, "Role of biomechanics in the understanding of normal, injured, and healing ligaments and tendons," *Sports Med Arthrosc Rehabil Ther Technol,* vol. 1, p. 9, 2009.

[38] M. Stubbs, *et al.*, "Ligamento-muscular protective reflex in the lumbar spine of the feline," *J Electromyogr Kinesiol,* vol. 8, pp. 197-204, Aug 1998.

[39] M. Solomonow, *et al.*, "The ligamento-muscular stabilizing system of the spine," *Spine (Phila Pa 1976),* vol. 23, pp. 2552-62, Dec 1 1998.

[40] S. Tozer and D. Duprez, "Tendon and ligament: development, repair and disease," *Birth Defects Res C Embryo Today,* vol. 75, pp. 226-36, Sep 2005.

[41] P. P. Provenzano, *et al.*, "Subfailure damage in ligament: a structural and cellular evaluation," *J Appl Physiol*, vol. 92, pp. 362-71, Jan 2002.

[42] C. Hurschler, *et al.*, "Scanning electron microscopic characterization of healing and normal rat ligament microstructure under slack and loaded conditions," *Connect Tissue Res*, vol. 44, pp. 59-68, 2003.

[43] K. M. Quapp and J. A. Weiss, "Material Characterization of Human Medial Collateral Ligament," *ASME Journal of Biomechanical Engineering*, 1997.

[44] L. M. Dourte, *et al.*, "Twenty-five years of tendon and ligament research," *J Orthop Res*, vol. 26, pp. 1297-1305, Oct 2008.

[45] M. J. Buehler, "Nature designs tough collagen: explaining the nanostructure of collagen fibrils," *Proc Natl Acad Sci U S A*, vol. 103, pp. 12285-90, Aug 15 2006.

[46] J. M. Aguilera and D. W. Stanley, Eds., *Microstructural Principles of Food Processing and Engineering*. USA: Aspen Publishers, Inc., 1999

[47] C. B. Frank, *et al.*, "Molecular biology and biomechanics of normal and healing ligaments--a review," *Osteoarthritis Cartilage*, vol. 7, pp. 130-140, Jan 1999.

[48] V. B. Duthon, *et al.*, "Anatomy of the anterior cruciate ligament," *Knee Surg Sports Traumatol Arthrosc*, vol. 14, pp. 204-13, Mar 2006.

[49] R. E. Debski, *et al.*, "Mechanical Testing of Tendons and Ligaments," in *Encyclopedia of Biomaterials and Biomedical Engineering*, G. L. Bowlin and G. W. Walsh, Eds., ed: Informa Healthcare, 2008, pp. 2583-2600.

[50] S. L. Woo, *et al.*, "Contribution of biomechanics, orthopaedics and rehabilitation: the past present and future," *Surgeon*, vol. 2, pp. 125-36, Jun 2004.

[51] S. C. Cowin, Ed., *Tissue Mechanics*. New York: Springer Science, 2007

[52] J. A. Weiss and J. C. Gardiner, "Computational modeling of ligament mechanics," *Crit Rev Biomed Eng*, vol. 29, pp. 303-371, 2001.

[53] J. A. Weiss, *et al.*, "Finite element implementation of incompressible, transversely isotropic hyperelasticity," *Computer Methods in Applied Mechanics and Engineering*, vol. 135, pp. 107-128, Aug 15 1996.

[54] J. F. Behrsin and C. A. Briggs, "Ligaments of the lumbar spine: a review," *Surg Radiol Anat*, vol. 10, pp. 211-9, 1988.

[55] C. Bonifasi-Lista, *et al.*, "Viscoelastic properties of the human medial collateral ligament under longitudinal, transverse and shear loading," *J Orthop Res,* vol. 23, pp. 67-76, Jan 2005.

[56] S. Hirokawa and R. Tsuruno, "Three-dimensional deformation and stress distribution in an analytical/computational model of the anterior cruciate ligament," *J Biomech,* vol. 33, pp. 1069-77, Sep 2000.

[57] J. C. Gardiner and J. A. Weiss, "Subject-Specific Finite Element Analysis of the Human Medial Collateral Ligament During Valgus Knee Loading," *J Orthopedic Research,* vol. 21, pp. 1098-1106, 2003.

[58] L. Yin and D. M. Elliott, "A biphasic and transversely isotropic mechanical model for tendon: application to mouse tail fascicles in uniaxial tension," *J Biomech,* vol. 37, pp. 907-16, Jun 2004.

[59] D. Hartright, "Biomechanical and Clinical Evaluation of Tendons and Ligaments," in *Orthopedical Biology and Medicene: Repair and Regeneration of Ligaments, Tendons and Joint Capsule*, ed Totowa, NJ: Humana Press Inc., 2006, pp. 185-99.

[60] S. L. Woo, *et al.*, "Effects of postmortem storage by freezing on ligament tensile behavior," *J Biomech,* vol. 19, pp. 399-404, 1986.

[61] M. Hayashi, *et al.*, "Influence of freezing with liquid nitrogen on whole-knee joint grafts and protection of cartilage from cryoinjury in rabbits," *Cryobiology,* vol. 59, pp. 28-35, Aug 2009.

[62] S. Giannini, *et al.*, "Effects of freezing on the biomechanical and structural properties of human posterior tibial tendons," *Int Orthop,* vol. 32, pp. 145-51, Apr 2008.

[63] D. Hartright and e. al., *Orthopedic Biology and Medicine: Repair and Regeneration of Ligaments, Tendons and Joint Capsule*. Totowna, 2006.

[64] T. Q. Lee and S. L. Y. Woo, "A New Method for Determining Cross-Sectional Shape and Area of Soft-Tissues," *Journal of Biomechanical Engineering-Transactions of the Asme,* vol. 110, pp. 110-114, May 1988.

[65] D. H. Kim, *et al.*, "Axial-scanning low-coherence interferometer method for noncontact thickness measurement of biological samples," *Appl Opt,* vol. 50, pp. 970-4, Feb 20 2011.

[66] F. Eckstein, *et al.*, "Non-invasive determination of cartilage thickness throughout joint surfaces using magnetic resonance imaging," *J Biomech,* vol. 30, pp. 285-9, Mar 1997.

[67] B. C. Fleming and B. D. Beynnon, "In vivo measurement of ligament/tendon strains and forces: a review," *Ann Biomed Eng,* vol. 32, pp. 318-28, Mar 2004.

[68] S. L. Woo, *et al.*, "Effects of knee flexion on the structural properties of the rabbit femur-anterior cruciate ligament-tibia complex (FATC)," *J Biomech,* vol. 20, pp. 557-63, 1987.

[69] F. A. Pintar, *et al.*, "Biomechanical properties of human lumbar spine ligaments," *J Biomech,* vol. 25, pp. 1351-1356, Nov 1992.

[70] S. M. Moore, *et al.*, "The glenohumeral capsule should be evaluated as a sheet of fibrous tissue: a validated finite element model," *Ann Biomed Eng,* vol. 38, pp. 66-76, Jan 2010.

[71] W. Sun, *et al.*, "Effects of boundary conditions on the estimation of the planar biaxial mechanical properties of soft tissues," *J Biomech Eng,* vol. 127, pp. 709-15, Aug 2005.

[72] S. L. Woo, *et al.*, "Mathematical modeling of ligaments and tendons," *J Biomech Eng,* vol. 115, pp. 468-73, Nov 1993.

[73] M. A. Puso and J. A. Weiss, "Finite element implementation of anisotropic quasi-linear viscoelasticity using a discrete spectrum approximation," *J Biomech Eng,* vol. 120, pp. 62-70, Feb 1998.

[74] A. J. M. Spencer, *Continuum Mechanics* Mineola: Dover Publications, 2004.

[75] K. M. Quapp and J. A. Weiss, "Material characterization of human medial collateral ligament," *J Biomech Eng,* vol. 120, pp. 757-63, Dec 1998.

[76] J. A. Weiss, "A constitutive model and finite element representation for transversely isotropic soft tissues," Department of Bioengineering, University of Utah, Salt Lake City, 1994.

[77] H. Yahia and N. Newman, "A light and electron microscopic study of spinal ligament innervation," *Z Mikrosk Anat Forsch,* vol. 103, pp. 664-674, 1989.

[78] R. Scapinelli, *et al.*, "The lumbar interspinous ligaments in humans: anatomical study and review of the literature," *Cells Tissues Organs,* vol. 183, pp. 1-11, 2006.

[79] G. Voena, "[Anatomical research on the structure of the intraspinal ligaments of the lumbar section of the spine in man]," *Biol Lat,* vol. 10, pp. 7-27, Jan-Mar 1957.

[80] D. J. Heylings, "Supraspinous and interspinous ligaments of the human lumbar spine," *J Anat,* vol. 125, pp. 127-131, Jan 1978.

[81] R. Scapinelli, "Localized ossifications in the supraspinous and interspinous ligaments of adult man," *Rays,* vol. 13, pp. 29-33, Jan-Apr 1988.

[82] T. Iida, *et al.*, "Effects of aging and spinal degeneration on mechanical properties of lumbar supraspinous and interspinous ligaments," *Spine J,* vol. 2, pp. 95-100, Mar-Apr 2002.

[83] G. Keorochana, Cyrus E. Taghavi, Shiau-Tzu Tzeng, Kwang-Bok Lee, Jen-Chung Liao2, Jeong Hyun Yoo, and Jeffrey C. Wang, "MRI classification of interspinous ligament degeneration of the lumbar spine: intraobserver and interobserver reliability and the frequency of disagreement," *European Spine Journal,* 2010.

[84] L. H. Yahia and N. Newman, "Innervation of spinal ligaments of patients with disc herniation. An immunohistochemical study," *Pathol Res Pract,* vol. 187, pp. 936-938, Dec 1991.

[85] J. M. Cavanaugh, *et al.*, "Sensory innervation of soft tissues of the lumbar spine in the rat," *Journal of Orthopaedic Research,* vol. 7, pp. 378-388, 1989.

[86] H. Jiang, *et al.*, "The nature and distribution of the innervation of human supraspinal and interspinal ligaments," *Spine (Phila Pa 1976),* vol. 20, pp. 869-876, Apr 15 1995.

[87] M. Sekine, *et al.*, "Mechanosensitive afferent units in the lumbar posterior longitudinal ligament," *Spine (Phila Pa 1976),* vol. 26, pp. 1516-1521, Jul 15 2001.

[88] G. Keorochana, *et al.*, "Magnetic resonance imaging grading of interspinous ligament degeneration of the lumbar spine and its relation to aging, spinal degeneration, and segmental motion," *J Neurosurg Spine,* vol. 13, pp. 494-9, Oct 2010.

[89] M. B. Dekutoski, *et al.*, "Pathologic correlation of posterior ligamentous injury with MRI," *Orthopedics,* vol. 33, p. 53, Jan 2010.

[90] S. H. Lee, *et al.*, "Soft stabilization with interspinous artificial ligament for mildly unstable lumbar spinal stenosis: a multicenter comparison," *Arch Orthop Trauma Surg,* vol. 130, pp. 1335-41, Nov 2010.

[91] F. Hartmann, *et al.*, "Biomechanical effect of different interspinous devices on lumbar spinal range of motion under preload conditions," *Arch Orthop Trauma Surg,* Dec 29 2010.

[92] C. S. Shim, *et al.*, "Biomechanical evaluation of an interspinous stabilizing device, Locker," *Spine (Phila Pa 1976),* vol. 33, pp. E820-7, Oct 15 2008.

[93] J. Senegas, *et al.*, "Long-term actuarial survivorship analysis of an interspinous stabilization system," *Eur Spine J,* vol. 16, pp. 1279-87, Aug 2007.

[94] J. B. Myklebust, *et al.*, "Tensile strength of spinal ligaments," *Spine (Phila Pa 1976),* vol. 13, pp. 526-531, May 1988.

[95] M. M. Panjabi, *et al.*, "Physiologic strains in the lumbar spinal ligaments. An in vitro biomechanical study 1981 Volvo Award in Biomechanics," *Spine (Phila Pa 1976),* vol. 7, pp. 192-203, May-Jun 1982.

[96] R. Putz, "The detailed functional anatomy of the ligaments of the vertebral column," *Ann Anat,* vol. 174, pp. 40-47, Feb 1992.

[97] R. L. Waters and J. M. Morris, "An in vitro study of normal and scoliotic interspinous ligaments," *J Biomech,* vol. 6, pp. 343-348, Jul 1973.

[98] R. Mitra, *et al.*, "Interspinous ligament steroid injections for the management of Baastrup's disease: a case report," *Arch Phys Med Rehabil,* vol. 88, pp. 1353-1356, Oct 2007.

[99] R. Maes, *et al.*, "Lumbar interspinous bursitis (Baastrup disease) in a symptomatic population: prevalence on magnetic resonance imaging," *Spine (Phila Pa 1976),* vol. 33, pp. E211-215, Apr 1 2008.

[100] J. R. Jinkins, "Lumbosacral interspinous ligament rupture associated with acute intrinsic spinal muscle degeneration," *Eur Radiol,* vol. 12, pp. 2370-2376, Sep 2002.

[101] M. Sharma, *et al.*, "Role of ligaments and facets in lumbar spinal stability," *Spine (Phila Pa 1976),* vol. 20, pp. 887-900, Apr 15 1995.

[102] S. M. McGill and V. Kippers, "Transfer of loads between lumbar tissues during the flexion-relaxation phenomenon," *Spine (Phila Pa 1976),* vol. 19, pp. 2190-2196, Oct 1 1994.

[103] Bradshaw R.J., *et al.*, "Spinal ligaments: Anisotropic characterization using very small samples," in *Proceedings of the SEM Annual Conf & Exposition on Experimental and Applied Mechanics,* Indianapolis, IN, 2010.

[104] M. Eskner and R. Sandstrom, "Mechanical Property Evaluation Using the Small Punch Test," *Journal of Testing and Evaluation,* vol. 32, pp. 1-8, 2004.

[105] J. C. Gardiner and J. A. Weiss, "Subject-Specific Finite Element Analysis of the Human Medial Collateral Ligament During Valgus Knee Loading," *J Orthopedic Research,* vol. 21, pp. 1098-106, 2003.

[106] K. J. Stabile, *et al.*, "Bi-directional mechanical properties of the human forearm interosseous ligament," *J Orthop Res,* vol. 22, pp. 607-612, May 2004.

[107] D. R. Einstein, *et al.*, "Dynamic finite element implementation of nonlinear, anisotropic hyperelastic biological membranes," *Comput Methods Biomech Biomed Engin,* vol. 6, pp. 33-44, Feb 2003.

[108] S. M. Renner, *et al.*, "Novel model to analyze the effect of a large compressive follower pre-load on range of motions in a lumbar spine," *J Biomech,* vol. 40, pp. 1326-32, 2007.

[109] F. Pietraszkiewicz and M. Tysiewicz-Dudek, "Epidemiology of spinal injuries in Lubuskie Province," *Ortop Traumatol Rehabil,* vol. 12, pp. 435-42, Sep-Oct 2010.

[110] M. J. Vives, *et al.*, "Spinal injuries in pedestrians struck by motor vehicles," *J Spinal Disord Tech,* vol. 21, pp. 281-7, Jun 2008.

[111] A. J. Schoenfeld, *et al.*, "Evaluation and management of combat-related spinal injuries: a review based on recent experiences," *Spine J,* Jun 1 2011.

[112] H. Yahia, *et al.*, "Structure-function relationship of human spinal ligaments," *Z Mikrosk Anat Forsch,* vol. 104, pp. 33-45, 1990.

[113] L. S. Matthews and D. Ellis, "Viscoelastic properties of cat tendon: effects of time after death and preservation by freezing," *J Biomech,* vol. 1, pp. 65-71, Jul 1968.

[114] S. Hasberry and M. J. Pearcy, "Temperature dependence of the tensile properties of interspinous ligaments of sheep," *J Biomed Eng,* vol. 8, pp. 62-6, Jan 1986.

[115] S. L. Woo, *et al.*, "The effects of strain rate on the properties of the medial collateral ligament in skeletally immature and mature rabbits: a biomechanical and histological study," *J Orthop Res,* vol. 8, pp. 712-21, Sep 1990.

[116] N. Yoganandan, *et al.*, "Geometric and mechanical properties of human cervical spine ligaments," *J Biomech Eng,* vol. 122, pp. 623-9, Dec 2000.

APPENDIX A. DESIGN SUMMARY

The design of the anisotropic small punch (ASPT) test involved a collaborative effort and several iterations of designing and prototyping. The concept and device were originally conceived by Dr. Anton Bowden in 2007. Development of a practical version of the ASPT has been an iterative process, which first began in 2007 with large scale ASPT versions. This initial development was done by Brent Showalter, Spencer Shore, and Alison Rankin. Subsequently, Dan Robertson and I focused on scaling down the device to applications of testing spinal ligaments. I was primarily responsible for generating the initial design concept and developing the associated experimental testing methods. Dan was heavily involved in machining iterative prototypes and developing the associated material characterization. Finally, in the 2010-2011 school year, a BYU capstone project was tasked with optimization of the ASTP setup. I was assigned as a liaison for the project and was consequently heavily involved in providing feedback throughout the design process. A summary of personal contributions throughout my time on this project is included in this appendix. An additional recommendation for future application is likewise included.

As previously stated in the body of this thesis, the principle motivation in designing the ASPT was to develop a multiaxial testing method, capable of testing very small samples, and suitable for maintaining the integrity of the biological samples. The delicate nature of the ligament tissue also required the implementation of sophisticated experimental and data collection techniques in order to accurately measure the material response.

Three major steps were executed to create and optimize the ASPT design. First, design objectives for the device were developed to initialize essential design processes and produce detailed generations of concept designs. Second, through a series of prototypes the systems and components of the ASPT were manufactured and assembled. Third, prior to testing the human spinal ligament samples, experimental techniques were developed using bovine Achilles tendons. The details of this process are discussed below.

A.1 Design Objectives

The design objectives established for this testing device included designing: (1) a suitable gripping methodology in which the sample integrity was maintained and no slipping occurred, (2) accurate measuring the force-deflection of a sample, and (3) capturing anisotropic profiles via optical systems. Concept designs went through a series of reviews to optimize design components, dimensions and capabilities.

First, to increase the quality of ligament fixation, a combination of techniques were employed. It was found that increasing the grip surface to sample volume ratio greatly reduced the tendency for the sample to slip. Consequently a circular sample was used, clamping the outer perimeter. To additionally enhance the mechanical hold, micro grips (~0.1mm) were etched onto the clamping surfaces of the device (See Figure A-1).

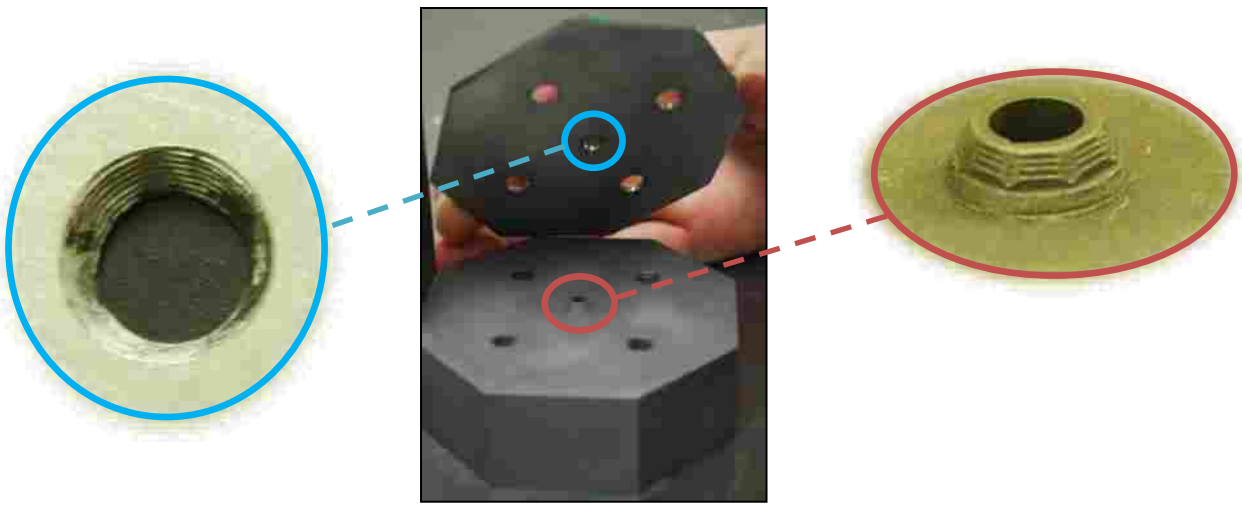

Figure A- 1. Zoomed images of micro grips: (Left) Top Plate (Middle) ASPT (Right) Etched Cone

A threaded lead screw was implemented for measuring displacement, which when turned actuated a 'piston' plunger and allowed measured displacements to be computed within ± 0.01 mm. Forces induced on the central indenter rod are measured with a 22 lbs load cell to an accuracy of ±0.005 lbs. Both systems were mounted inferior to the apparatus. The force and displacement of the plunger reflects the force and displacement experienced by the tissue sample at the point of contact. It was essential to use extremely accurate methods to simultaneously capture this information, as the sample has a very small radius (1.8 mm). Potential sources of noise in the systems were identified and reduced as much as possible.

Obtaining anisotropic displacement profiles of test samples required that video images be obtained simultaneous by two orthogonally placed CCD cameras (scA640-70fm Basler Vision Technology) mounted with macro zoom lenses (MLH-10X, Computar, New York). These two cameras were oriented so as to capture the anisotropic response of the collagen fibers along the longitudinal (parallel) and transverse (perpendicular) directions Capturing orthogonal slope profiles, of the multiaxial setup, was also essential to qualitatively understanding the mechanics

associated with an anisotropic material in a circular punch. Likewise a superiorly placed microscope (CM1-USB microscope) recorded necessary imaging data to ensure that test samples were adequately clamped and that no localized slipping occurred throughout the testing process. Finally, these optical systems were synchronized with data collection systems in synchronized in a custom Labview program (Labview, version 9.0, National Instruments, Austin).

A.2 Final Design

The manufactured device rendered a biomechanical testing method which accomplished the established design objectives, was successfully manufactured and assembled, and subsequently used to validate experimental punch test protocols. The Labview code integrates video from the two CCD cameras with synchronized data files of indenter rod force and displacement with respect to time. As shown in Figure 3-5 the force varies with time and each sample is unique in its response. The complete test setup is shown in Figure A-2.

A.3 Experimental Techniques

The experimental methodology was polished though a series of testing using bovine achilles tendon. Various methods were employed to acquire samples of appropriate thickness. It was found that sample with an approximate thickness of 1 mm were consistently less likely to slip, due to excess volume, and were also less likely to tear during testing. To achieve thickness representative of the ISL bovine samples were cut on a meat slicer while freshly frozen, to 3-5 mm in thickness. Next to acquire the desired thickness samples were cut with microtome blades. Also to ensure sample quality samples were hydrated with a saline solution at 10 minute

intervals. Once a sample was at an appropriate thickness the thickness was measured and confirmed to have a consistent cross section via the calibrated ASPT optical systems. Prior to testing, each sample was aligned along the predominant collagen direction, such that the longitudinal and transverse responses were captured by the two orthogonal CCD cameras. The sample was then preconditioned to negate viscoelastic effects by vertically displacing the indenter rod at 0.2 mm for 10 cycles. The load cell and potentiometer was then quickly recalibrated. Finally, the sample was tested by displacing the indenter rod at a rate of 2 mm/s until sample failure. Indenter rod force and deflection were measured respectively via the 22 lbs load cell and potentiometer with accuracies of ± 0.005 lbs and ± 0.01 mm. The implementation of these steps insured the applied experimental procedures and refined optical and numerical data techniques were capable of characterizing the ISL.

Microtome blades were found to be most helpful in accurately sectioning the samples to consistent thicknesses, regardless of the initial specimen size. The slippery nature of the ISL required caution in handling and gripping samples in the ASPT setup. Generally, when test samples had little surface area to grip or were greater than 2 mm in thickness they would usually slip during testing. One aspect that was not a primary focus of the study was recording the geometry variation of ISL throughout its entire dimensions. Focus on this would allow a more detailed study of patterns of the inhomogeneities which exist in the ISL. Likewise this subject has not been investigated in detail, in the literature, to our knowledge. We also suggest strongly suggest using a higher data collection rate for force-deflection data, to display a detailed force-deflection curve. Although this did not cause great disparity in the acquired results it would allow remove experimental noise within the ASPT and would result in higher R^2 values when characterizing samples in the optimization. Finally, testing the ISL specimens for a whole spine

would have been ideal for this study. The spines that were tested during the present work were previously subject to other types of testing within the lab and consequently had gone through two freeze thaw cycles and other mechanical loading. This was assumed to not affect the end results, based on literature investigating these effects on soft tissue as negligible for several freeze-thaw cycles [60, 113-115]. Similar to other studies, one aspect that may be interesting to investigate would be to conducting testing of ISL specimens that have been freshly removed during surgical procedures and potentially have different characteristics [78, 97].

A.4 Raw Data

As stated in the publication a total of 42 individual test samples were characterized, however only averages of the material parameters were reported in the publication, similar to previously published work characterizing ligament properties [69, 94, 116]. However, the full dataset is provided here in anticipation that these additional results may be useful at some point in the future. Consequently, the material parameters for all test samples are presented in Table A-1.

Table A - 1 Summary of all ISL test samples and the derived material parameters

ID	Level	n	c_1	c_3	c_4	c_5	λ*	R^2	t (mm)
A	L2-L3	1	0.19	0.18	30	30.69	1.08	0.9958	1.32
	T12-L1	1	0.43	0.1	1.1	9.84	1.1	0.9927	1.35
B	L1-L2	1	0.29	0.1	1.1	20.63	1.1	0.9937	0.5
		2	0.5	1.43	18.45	40	1.1	0.989	0.78
		3	0.056	0.005	10.81	3	1.03	0.906	1.81
		4	0.18	0.32	1.1	6.03	1.06	0.9674	0.84
		5	0.16	0.45	10.75	39.12	1.05	0.999	1.17
	L2-L3	1	0.18	0.09	3.43	18.34	1.06	0.9986	2.14
		2	0.26	0.01	1.89	8.37	1.1	0.9796	1.24

Table A-1 Con't

ID	Level	n	c_1	c_3	c_4	c_5	λ*	R^2	t (mm)
B	L2-L3	3	0.176	0.684	12.3	10.69	1.11	0.97	0.84
		4	0.39	0.46	26	39.99	1.1	0.9725	0.84
		5	0.49	0.32	5.68	32.67	1.02	0.996	0.64
		6	0.24	1.46	12.03	24.97	1.09	0.9962	0.86
	T12-L1	1	0.5	0.19	35	5	1.09	0.947	0.64
		2	0.25	0.32	29.23	39.56	1.08	0.9978	0.86
C	L2-L3	2	0.07	0.9	13.37	25.21	1.1	0.9868	1.58
		3	0.5	2	12.8	12.85	1.1	0.9926	1.23
		4	0.23	0.01	7.43	18.08	1.07	0.9988	1.24
	L3-L4	1	0.3	0.01	8.27	6.96	1.1	0.9808	0.61
D	L2-L3	1	0.34	0.88	9.63	5	1.01	0.9776	0.74
		2	0.33	0.01	2.28	3	1.17	0.96	1.06
	T11-T12	1	0.43	0.19	29.9	39.9	1.09	0.9859	1.16
		2	0.19	0.72	1.1	27.13	1.05	0.9992	1.11
		3	0.33	0.99	18.49	21.41	1.1	0.9815	0.73
E	T11-T12	1	0.22	0.088	10.68	20.31	1.15	0.996	0.86
		2	0.32	2	10.68	33.59	1.15	0.998	0.72
		3	0.29	0.22	22.1	45	1.15	0.998	0.72
	T12-L1	2	0.206	0.616	30	45	1.07	0.993	0.62
F	L1-L2	1	0.13	0.01	13.28	11.22	1.1	0.9857	1.42
		2	0.5	1.22	30	7.05	1.04	0.984	0.79
		3	0.1	0.59	19.58	16.35	1.1	0.9952	0.9
	L3-L4	1	0.04	1.24	2.88	10.44	1.1	0.997	1.94
		2	0.22	0.15	7.76	8.96	1.06	0.9929	1
		3	0.07	1.58	3.28	5	1.1	0.9578	1.13
		4	0.39	1.2	20.39	17.65	1.05	0.9867	1.55
	L4-L5	3	0.41	0.3	1.1	10.84	1.1	0.9837	0.33
		4	0.33	0.27	25.93	6.79	1.1	0.9951	1.01
		5	0.13	0.67	1.1	5.17	1.01	0.9148	1.46
		6	0.2	0.58	4.76	14.67	1.1	0.9964	0.84
	T10-T11	1	0.384	1.397	16.577	35.18	1.1	0.995	0.8
		2	0.103	0.851	19.84	45	1.11	0.9991	0.68
		3	0.101	1.026	15.188	16.873	1.082	0.999	0.95